Örebro Studies in Technology 103

Joakim Larsson

Have you heard about wire?

Monitoring of the wire drawing process

Author: Joakim Larsson
Title: Have you heard about wire?, Monitoring of the wire drawing process

Publisher: Örebro University, 2024
www.oru.se/publikationer

Print: Örebro University, Repro 03-2024
ISSN: 1650-8580
ISBN: 978-91-7529-545-9 (print)
ISBN: 978-91- 7529-546-6 (pdf)

Abstract

Wire made from metal is a fundamental component found in almost every complex product, ranging from a simple pen to a spacecraft. It is used to manufacture nails, screws, springs, rivets, cables, welding electrodes, and numerous other items that surround us daily.

In an era characterized by increased environmental concerns and the pressing need for the industry to become more sustainable, process monitoring has emerged as a key instrument for strengthening the sustainability improvements of diverse industries and operations. Many industries have transitioned into the realm of Industry 4.0, entering an era of digital transformation and data-driven decision-making. However, the production of steel wire has fallen behind. The wire drawing process has been performed in a similar manner for the last century and the production machines generally lack advanced monitoring systems. To catch up, there is a great need to digitize the wire drawing process and that is the focus of this thesis, *Monitoring of the wire drawing process.*

In this thesis several different methods to monitor the wire drawing process are developed and evaluated, resulting in a process monitoring system for the wire drawing process.

Keywords: Wire drawing, process monitoring, condition monitoring, drawing force, performance monitoring

Table of Contents

Introduction 6
1.1 Motivation 6
1.2 Industrial and scientific questions 7
1.3 Methodology 7
1.3.1 Research methodology 7
1.3.2 Laboratory experimental setup 9
1.3.3 Evaluation of developed monitoring methods 10
1.4 Publications 11
1.5 Thesis structure 15
2 Fundamentals of wire drawing 16
2.1 Tools for wire drawing 16
2.1.1 Tool wear in wire drawing 19
2.2 Lubrication in wire drawing 20
3 Wire drawing theory 23
3.1 Drawing force 23
3.2 Temperatures 26
3.2.1 Wire temperature 26
3.2.2 Wire – Die surface contact temperature 27
3.2.3 Die temperature 28
4 Process problems affecting productivity and sustainability 30
4.1 Increased tool wear 30
4.2 Surface defects and wire breaks due to poor lubrication 31
5 Monitoring of the wire drawing process 33
5.1 Previous work 33
5.1.1 Resistance between die and wire 33
5.1.2 Vibration measurement 34
5.1.3 Temperature related measurements 34
5.2 Investigated monitoring methods 35
5.2.1 Vibration measurement 36

5.2.1.1 Development of method to measure and analyze vibrations in the wire drawing process 37
5.2.2 Wire temperature measurement 38
5.2.2.1 Development of method to use the temperature of the drawn wire for in-situ measurement of lubrication performance 39
5.2.2.2 Development of thermal imaging method 40
5.2.3 Wire brightness measurement 41
5.2.3.1 Development of a method to measure and analyze the brightness of drawn wire in-line 42
6 Results and discussion 45
6.1 Investigation of theoretical methods to evaluate the friction coefficient 45
6.2 Vibration measurements 51
6.3 Wire temperature measurements 57
6.4 Brightness measurements 65
6.5 Multiple sensor approach - WiSE 68
6.5.1 Results 72
7 Conclusions 79
7.1 General conclusions and future work 79
7.2 Answers to specific industrial and research questions 79
8 Acknowledgements 81
9 References 82

Introduction

1.1 Motivation

Wire made from metal can be found in almost every complex product, ranging from a simple pen to a spacecraft. Wire is used to manufacture nails, screws, springs, rivets, cables, welding material and many other things that surround us daily. Wire forms joints in our structures, stabilizes our tires and transports electricity. Without wire the world would not be the same. Wire has been an important part of society for a long time, the first known mentioning of wire and how it can be manufactured is found in the Bible (Old Testament), "And they did beat the gold into thin plates and cut it into wires" [1].

Today the production industry faces high demands on increasing sustainability and productivity. The production of steel wire has been performed in a similar manner for the last decade. Many other continuous process industries are moving into Industry 4.0, but the wire drawing industry is somewhat lagging. Industry 4.0 creates great demands in terms of measuring, understanding and being able to control the production process. To control and optimize a process it is necessary to know the current state of the process. Today, there is rarely any process monitoring in the wire drawing process. These demands provide the driving force for carry out the studies in this doctoral thesis, *Monitoring of the wire drawing process*.

Wire drawing is a continuous metal forming process where several tons of wire can be produced in each production run. Today it is not common to use a monitoring system to ensure the quality of the produced wire product in-line, and even if some kind of monitoring is performed it is rarely used to adjust or stop the process if problems occur. When a production run is finished the quality of the produced wire is checked, and if the wire is bad the whole batch of wire needs to be scrapped. By introducing repeatable and continuous monitoring of the process performance, it would be possible to detect problems before they become issues that lead to damage on the wire and the tools, leading to a more sustainable wire production.

1.2 Industrial and scientific questions

The industrial need is to be able to identify problems in the wire drawing process, to decrease the environmental impact and increase the productivity and profitability. In order to assist in this endeavor, the following questions have been investigated.

- Is it possible to detect problems in the wire drawing process by using process monitoring that can be implemented in an existing industrial wire drawing machine?
- Can problems be detected before they become an issue?
- Can the efficiency of the process be estimated using sensors?

The scientific questions are more related to understanding how different parameters affect the wire drawing process and how this can be measured.

- Are there measurable process parameters in the wire drawing process that reflect the properties of the produced wire?
- Can process signals be linked to material characteristics?

1.3 Methodology

1.3.1 Research methodology

The research conducted in this doctoral thesis is oriented towards the scientific philosophy of experimentalism. Quantitative experimental studies have been performed to give answers and understanding of hypotheses derived from the research questions.

The research questions formulated in the thesis are a direct reflection of the industrial needs. Many of the studies performed related to this thesis have been in close collaboration with the Swedish wire drawing industry, ensuring high relevance to the industry.

To identify what has been studied in the specific research topics previously, systematic literature reviews [2]–[4] of the research areas have been carried out. From these literature studies, knowledge gaps were identified, and hypotheses were set to try to fill these knowledge

gaps. Most of the studies included in this thesis have been published and are peer-reviewed, meaning that the work has contributed to the scientific field of wire drawing.

To investigate each set hypothesis, quantitative studies were performed. Both laboratory and industrial wire drawing experiments have been used for collecting empirical data. In the laboratory setting a controlled environment is achieved and there are also greater possibilities to measure the process conditions, which is necessary to get a good first evaluation of the hypothesis. If the results from the laboratory experiments were promising, the hypothesis was then further tested in an industrial setting, this approach makes implementation of the results on an industrial scale easier since the findings already have been tested in the correct environment. To gain more information from the experiments, characterization of the material (wire, tools and lubricant) used in the experiments has been performed using methods such as tensile tests, 3-dimensional measuring (CMM), scanning electron microscopy (SEM), hardness measurements and surface measurements.

The results have been processed using statistical methods, to ensure that the results were statistically significant. In several of the performed studies, finite element modeling was used give further understanding of the studied phenomena. Data from the experiments (geometries, forces, temperatures, and material properties) were used in the models as boundary conditions and to validate the model against the real process.

The research methodology described above and used in this thesis is in accordance with the steps seen in the flow chart presented in *Figure 1.1*. The methodology is inspired from research methodologies described by Agnew and Pyke, and Säftsten and Gustavsson [5], [6].

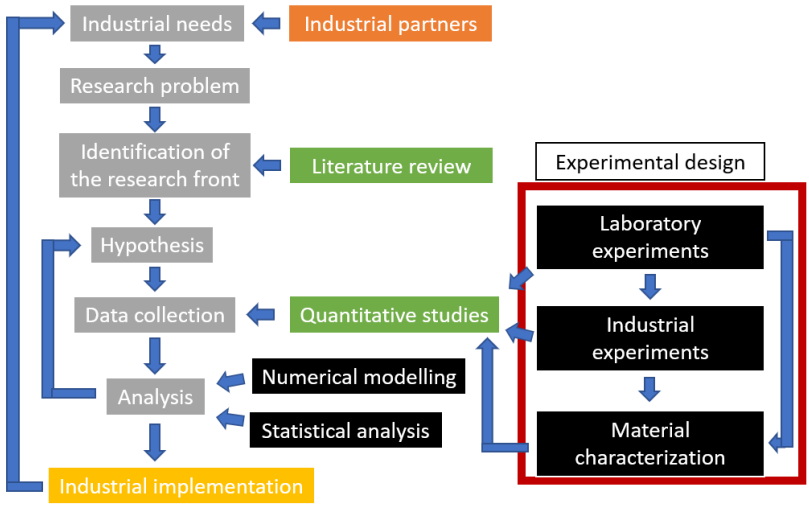

Figure 1.1. Research methodology flow chart showing the process used in the studies presented in this doctoral thesis.

The focus area of this doctoral thesis is production of steel wire using a dry lubricated wire drawing process, meaning that the findings are only validated for this process. Many of the findings may be applicable to other types of drawing or rolling processes, but this remains to be investigated in the future.

1.3.2 Laboratory experimental setup

In the studies included in this thesis, wire drawing experiments have been conducted in the research wire drawing line at Örebro University. This has been done because it is vital to have a controlled process when performing initial investigations. An industrial setup is also preferred so the investigated methods can be implemented in the real environment. However, for the first evaluation the level of uncertainties in the industrial process line is often too high, and the well-controlled laboratory environment is to be preferred.

The laboratory setup at Örebro university includes a driven rotating pay off, which supplies the wire with an even resistance, which is very important when evaluating drawing force. The wire is drawn by a single block wire drawing machine without a spooler, the wire is stored at the capstan, so a maximum of around 100 kg of wire can be used in an experiment. The base setup of the machine includes measurement of drawing force, drawing speed, wire temperature, ambient temperature and moisture. The parameters are recorded, filtered and synced in a LabVIEW [7] software developed by the author. The research drawing line is shown in *Figure 1.2*.

Figure 1.2. Research wire drawing line at Örebro university.

1.3.3 Evaluation of developed monitoring methods

In this thesis, methods for monitoring the wire drawing process are developed and evaluated. This is therefore the focus of most of the publications in the thesis. The evaluation method used throughout the papers is quite similar and aims at evaluating the correlation between the investigated process monitoring method, the status of the wire drawing process, the characteristics of the produced wire and a recognized in-situ evaluation method (drawing force). To ensure the best possible control of the process, these evaluations have been

carried out using the laboratory experimental wire drawing setup presented in chapter 1.3.2.

To change the status of the wire drawing process, the lubrication state of the process was changed by removing the lubricant to achieve lubricant starvation leading to a non-working process. Meaning that the evaluation experiments start with a well-functioning process which is then transformed into a non-working process without stopping the process.

1.4 Publications

This thesis is based on the following studies, referred to in the text by their Roman numerals. It contains three journal papers, one conference paper and one submitted manuscript. The following list contains the included papers and the author's contributions:

- **Paper I**
  Joakim Larsson, Rachel Pettersson & Christer Korin. *Experimental and theoretical examination and development of methods to calculate required pull force in wire drawing.* Manuscript to be published in Heliyon. Author's contributions: Methodology, Conceptualization, Investigation, Writing of original draft.

- **Paper II**
  Lars Pejryd, Joakim Larsson & Mikael Olsson. (2017). *Process monitoring of wire drawing using vibration sensoring.* CIRP - Journal of Manufacturing Science and Technology, 18, pp. 65-74. Author's contributions: Methodology, Conceptualization, Investigation, Writing of parts of original draft.

- **Paper III**
  Joakim Larsson, Anton Jansson & Patrik Karlsson. (2019) *Monitoring and evaluation of the wire drawing process using thermal imaging.* The International Journal of Advanced Manufacturing Technology, 101 (5-8), pp. 2121-2134. Author's contributions: Methodology, Conceptualization, Investigation, Writing of original draft.

- **Paper IV**
  Joakim Larsson, Anton Jansson & Lars Pejryd. (2017). *Process monitoring of the wire drawing process using a web camera based vision system.* Journal of Materials Processing Technology, 249, pp. 512-521. Author's contributions: Methodology, Conceptualization, Investigation, Writing of original draft.

- **Paper V**
  Joakim Larsson, Patrik Karlsson & Anton Jansson. (2023) *In-situ evaluation of the performance of wire drawing using multiple sensors*. In: In: Wire Association International 93rd Annual Convention, Atlanta, 9-11/5 2023. Author's contributions: Methodology, Conceptualization, Investigation, Writing of original draft.

The following publications have also been published in the same research area as the above presented papers by the author of this thesis, but are not included in the thesis:

- Joakim Larsson & Magnus Jarl. (2011). *Teknik för högre draghastigheter: temperaturens inverkan.* In: Nordic wire drawing associations annual conference, Sundsvall, Sweden, 15-16/9 2011, pp. 53-66.

- Joakim Larsson & Magnus Jarl. (2012). *Högre draghastighet.* In: Nordic wire drawing associations annual conference, Hagen, Germany, 18-19/9 2012. pp. 63-70.

- Joakim Larsson, Helena Johansson-Cider & Magnus Jarl. (2013). *Monitoring of the wiredrawing process.* In: Wire Association International 83rd Annual Convention, Atlanta, 22-25/4 2013.

- Joakim Larsson, Helena Johansson-Cider & Magnus Jarl. (2014). *Temperatures in the wiredrawing process: Measurements and simulations.* Wire Journal International, 47 (2), pp. 128-133.

- Joakim Larsson & Lars Pejryd. (2015). *Preliminära resultat från jämförelse mellan konventionell dragning och dragning med Roller Dies.* In: Nordic wire drawing associations annual conference, Ed, Sweden, 24-25/9 2015, pp. 103-111.

- Joakim Larsson. (2016). *Vibrationsmätning som processövervakning i tråddragningsprocessen*. In: Nordic wire drawing associations annual conference, Åbo, Finland, 22-23/9 2016, pp. 53-59.

- Lars Pejryd & Joakim Larsson. (2018). *Additively manufactured tool holder for wire drawing processes.* In: Euro PM 2018 Congress and Exhibition, Bilbao, Spain, October 14-18, 2018.

- Karim El-Amine, Joakim Larsson & Lars Pejryd. (2018). *Experimental comparison of roller die and conventional wire drawing*. Journal of Materials Processing Technology, 257, pp. 7-14.

- Joakim Larsson. (2019). *Digitalisering i tråddragningsindustrin.* In: Nordic wire drawing associations annual conference, Loka, Sweden, 19-20/9 2019, pp. 66-72.

- Joakim Larsson, Anton Jansson & Lars Pejryd (2020). *Wire 4.0* Wire Journal International,

- Joakim Larsson, Patrik Karlsson & Lars Pejryd. (2020). *The effect of bearing length on the surface quality of drawn wires*. Wire Journal International, 53 (2), pp. 50-55.

- Joakim Larsson, Patrik Karlsson, Jens Ekengren & Lars Pejryd. (2021). *Enhanced Cooling Design in Wire Drawing Tooling Using Additive Manufacturing.* In: The 2nd International Conference on Additive Manufacturing for Products and Applications (AMPA 2020), Zürich, Switzerland, 1-3/9 2020. pp. 426-436.

- Kumar Surreddi, Joakim Larsson & Mikael Olsson. (2022). *Investigating the surface degradation and wear mechanisms of uncoated and PVD-coated cemented carbide dies in steel wire drawing.* In: 12th Tooling Conference & Exhibition Proceedings. (TOOling 2022), Örebro, Sweden, 25-27/4 2022. pp. 523-530.

- Joakim Larsson, Sara Garmendia Alustiza, Nagore Otegi & Patrik Karlsson. (2022). *Enhanced cooling by conformal cooling of additively manufactured wire drawing tools made of cemented carbides.* In: Metal Additive Manufacturing Conference (MAMC 2022), Graz, Austria, 26-28/9 2022. pp. 225-235.

- Joakim Larsson, Bogdan Chetroiu & Erik Enghag. (2022). *Additively manufactured conformal cooling tool holder for wire drawing utilizing triply periodic minimal surfaces.* In: 12th Tooling Conference & Exhibition (TOOling 2022), Örebro, Sweden, 25-27/4 2022. pp. 22-29.

- Joakim Larsson. (2023). *Cooling in tooling – Case studies from the wire drawing industry* In: Wire & Cable Milan 2023, Milano, Italy, 16/10 2023. pp. 73-82.

1.5 Thesis structure

Chapter 1 introduces the topic and the motivation behind the work. The overarching questions that the thesis tries to answer are presented.

Chapter 2 contains an introduction to the wire drawing process.

Chapter 3 introduces the theories behind wire drawing.

Chapter 4 gives an overview of what type of problems which might be possible to identify using process monitoring.

Chapter 5 turns the attention to the main area of this thesis, monitoring of the wire drawing process.

Chapter 6 present and discusses the results from the research studies included in the thesis.

Chapter 7 finally concludes the thesis and answers the overarching questions.

2 Fundamentals of wire drawing

In this chapter the fundamentals of wire drawing are presented, what is wire drawing and what are the important factors for the process to work.

Wire drawing is a process whereby a hot rolled wire is refined by forcing the wire through a single or a series of tools (see *Figure 2.1*). In these tools the cross-section of the wire is reduced, making the wire longer and stronger, due to the continuous volume and deformation hardening. Using this method high dimensional tolerances of the cross-section can be achieved. The deformation leads to high pressures acting between the tool and the wire which can lead to immense frictional forces in the drawing direction. Therefore, to make the process work, it must be well lubricated. Issues with the lubrication can lead to increased tool wear, surface damages and other problems which all lead to a decrease in productivity and lower yield from the production process, which is not good for sustainability. Many different types of metals can be processed using wire drawing and many different types of lubricants can be used. However, in this thesis the focus is on steel wire being lubricated with soap-based powder lubricant.

2.1 Tools for wire drawing

From the beginning round wire was made using a hammer, forging the wire into the desired shape, however, those who have tried forging something into a round constant shape know that this is very difficult. The next step of the development of the wire drawing process was to use tools to deform the wire, leading to more consistent shape of the produced wire. The first types of tools that was used for drawing wire were stones with conical holes. Archaeologists have found drawing stones as old as from 200 B.C [8]. As we learned more about how to manufacture hard materials, the choice of the material used for the drawing tool changed, also the shape of the tool, from the beginning a plate with a series of holes were used, as the process evolved and the wire no longer was drawn by hand but by a

machine, a tool with a single hole was developed, these tools are normally referred to as drawing dies.

A common material used in the drawing dies before the 1900's was hardened steel, which is still used today for some special applications. However, for most applications, materials with superior hardness are commonly used for the drawing dies. These harder materials were introduced during the first half of the 1900's. Drawing tools made of diamond were first introduced and a bit later tool makers also started to use cemented carbide for the drawing dies, today these two materials are still the ones most commonly used [8]. Both natural, polycrystalline, and manufactured monocrystalline diamonds are used, and they give different properties to the produced wire. Cemented carbide dies are normally made from tungsten carbide with a cobalt binder (6-10%). These are used for a wide span of wire diameters and have a lower cost compared to diamond dies. Diamond dies are usually used for smaller dimensions of wire (<3 mm) due to the cost which increases exponential as the die core needs to be bigger. The life span of the different types of tools varies vastly, depending on the production planning, the tool life can be a crucial factor for the profitability of the production process. In recent years, a lot of efforts have been made to increase the life of cemented carbide dies, research has included using coatings on the functional surfaces of the drawing die [9]–[13].Today many die suppliers are starting to supply coated dies [14]–[18]. Another attempt to improve the life-time of the die has been to improve the cooling of the drawing die, which has shown great potential, but is not yet fully implemented by the industry [19]–[23].

Nevertheless, even if a coating or super-efficient cooling is used, the inner shape of the die, which forms the wire, is always of highest importance to achieve an efficient process and a sufficient tool life. This shape has evolved over time and many researchers have done work on optimizing this geometry [24]-[34], however, there are still a lot of different opinions how the optimal drawing die should look like. Despite this, the general geometrical features of the drawing are the same for all modern drawing dies. These features are important for the efficiency of the drawing process and also have an impact on

the resulting mechanical properties of the drawn wire. A schematic of a drawing die is shown in *Figure 2.1*.

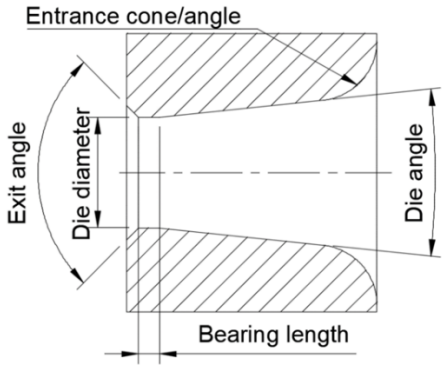

Figure 2.1. Schematic drawing die, showing the most important geometrical features.

The wire enters the die from the right and the first part of the die is called entrance angle/cone/radius. The sole purpose of this first part is to collect the lubricant, so it can follow the wire into the drawing die. The wire starts to deform as it comes in contact with the angled surface called the die angle, which is normally referred to as 2α, drawing dies ranging from 6-24° can be found as standard products from most suppliers [15], [17], [18], [35].

The die angle and the diameter of the die are the two parameters that are usually possible to specify when buying drawing dies. The die angle has a large impact on the deformation of the wire, meaning that it affects the mechanical properties of the drawn wire [36]. After the die angle, the drawing die has a straight part, the bearing, it is here that the diameter and roundness of the wire is set, so it is of highest importance for the drawing process. The length of the bearing will also affect the process and the finished product [25], [27], [33], [37]. After the bearing, is the exit angle. The purpose of this cone is to make it easy for residual lubricant to escape from the drawing die.

The die geometry also has a large impact on how efficient the lubrication will be, more on this in chapter 2.2.

2.1.1 Tool wear in wire drawing

As for most other tools, the dies wear as they are used and wire passes through them. As the die wears, the produced wire will go out of dimensional tolerance. When this occurs, the dies needs to be changed, which can be a time consuming activity decreasing the productivity [38]. So, to increase the productivity, it is important to achieve as low wear rate as possible for continuous wire production. Also, as mentioned in section 2.1, since a large proportion of the used tools contains cobalt, decreasing the tool wear will increase the sustainability since less die material will be used.

Tool wear is a phenomenon which has been studied for a long time. A model of how materials wear in contact with each other was first developed by Archard [39]

$$W = \frac{V}{L} = \frac{k_f F_n}{3H}, \quad (1)$$

where W (mm^3/m) is the worn volume per sliding distance, V is the total removed volume, L is the total sliding distance, k_f is a constant relating to the materials involved and the friction condition between them, F_n is the normal pressure (which is related to the drawing force) and H is the hardness of the tool.

Even though the wear of drawing dies has high importance to the wire drawing process and a crucial impact on the profitability of the process, not many research studies have been conducted on the subject. There have been many different approaches on how the wear of the drawing dies can be predicted.

Wistreich studied the wear of drawing dies and arrived at the conclusion that most of the wear occurs where the wire first comes into contact with the die angle and that there is some wear in the die angle but not so much in the bearing area. This wear leads to the creation of a geometrical torus, visible to the human eye in the beginning of the die angle. He also concluded that the wear is of the abrasive type [40].

Kim et al used finite element analysis to understand the wear in the drawing process [41]. The researchers used Archard's wear equation

and adapted it for wire drawing. Since the contact pressure will vary in the tool the equation should be written as

$$W = \sum_{i=1}^{N} \frac{k_f}{3H}(\sigma_n V_s \Delta t), \quad (2)$$

where σ_n is the normal stress acting on the die surface, V_s is the drawing speed, N is the time step number and Δt is the time step.

Enghag derived an equation for calculating the average relative pressure in the drawing die [36]. He did this by combining the equation for drawing force derived by Siebel and Kobitzsch [42] and the equation for average die pressure derived by Sachs [43]

$$\frac{q_d}{\sigma_w} = \left(-ln\left(1 - \frac{A_0 - A}{A_0}\right)\left(1 + \frac{\mu}{\alpha}\right) + \frac{2\alpha}{3}\right) \frac{1 - \left(\frac{A_0 - A}{A_0}\right)}{\left(\frac{A_0 - A}{A_0}\right)\left(1 + \frac{\mu}{tan\alpha}\right)}, \quad (3)$$

where A_0 and A_1 are the cross-sectional area of the wire before and after the reduction, q_d is the average die pressure, σ_w is the average flow stress in the drawn wire and μ is the coefficient of friction between the wire and the die.

Common for the above equations is that they indicate that the friction has an impact on the wear of the drawing dies, meaning that it is important to always assure a well-functioning lubrication of the wire drawing process.

2.2 Lubrication in wire drawing

Lubrication is crucial for the wire drawing process to work, the die and the wire must be separated from metallic contact with each other for the process to work efficiently. However, this is not always the case. The lubrication type studied in this thesis is what is commonly referred to as dry drawing (not to be confused with the lubrication state dry which a term often used in tribology), where a dry soap-based powder lubricant is used.

In wire drawing, there are four possible lubrication states, hydrodynamic, mixed, boundary and dry[36], [44]. In hydrodynamic

lubrication there is a thick lubrication film that separates the die from the wire, in boundary lubrication there is a thin film of lubrication that does not completely protect the process from metallic contact and in mixed lubrication there is both boundary and hydrodynamic lubrication. In dry lubrication there is constant metallic contact between the die and wire. *Figure 2.2* shows schematic images showing these lubrication states.

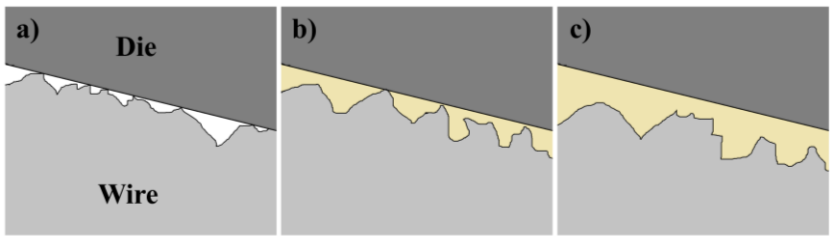

Figure 2.2. Lubrication states occurring in wire drawing. a) Dry b) Boundary c) Hydrodynamic

These three different lubrication states lead to differences in process efficiency, tool wear and drawn wire properties. The dry state leads to immense tool wear and damaged surfaces and should be avoided in a normal drawing process.

The lubricant is fed to the reduction process by the wire itself, the wire passes through a box filled with lubricant and drags the lubricant (calcium- or sodium-based powder) into the drawing die. The amount of lubricant that is dragged into the process is dependent on many parameters such as the surface of the wire, the presence and properties of lubricant carrier, the geometry of the die, the shape and size of the lubricant particles and others.

As the wire gets closer to the deformation zone a wedge-shaped void is created between the wire and the die, where the wire first comes in contact with the die surface. The shape of this void determines how much lubricant will be sucked into the deformation zone. A smaller die angle will create longer and tighter cone, which can improve the lubrication. However, this can also lead to an unstable drawing process, if the wire does not enter the die perfectly straight, it might

come in contact with one side of the die already in the beginning of the die angle, long before it reaches the deformation zone. If this occurs, that side of the wire will not be fully lubricated, creating problems in the drawing process. It is common to have larger die angle in the first draw of a drawing series, this is to compensate for the wire rod not being perfectly straight.

The demand in the industry to increase productivity results in a need to increase the drawing speed. However, this may cause problems in the lubrication process: as the speed is increased, more frictional and deformation heat per time unit will be generated in the drawing die, leading to higher temperatures. The functionality of the lubrication in the wire drawing process is highly dependent on the temperature. Melting intervals for dry lubricants, have been studied using differential scanning calorimetry (DSC), thermogravimetric analysis (TGA) and thermomechanical analysis (TMA) [36], [45], [46]. However, in general, the overall common knowledge of the dry lubricants used in the wire drawing process is today limited. The world market is dominated by a few lubricant manufacturers, who are secretive about the chemical composition and the specific functions of the components in the individual lubricants. Knowledge is empirical and often based on trial-and-error experiments performed directly at wire drawing companies. This lack of understanding of the lubrication process creates even greater demands on being able to measure and verify that a well-functioning lubrication process is achieved at all times.

3 Wire drawing theory

This chapter presents the theoretical aspects of wire drawing. Methods to estimate the required force to pull the wire and temperature increases are presented and explained.

3.1 Drawing force

The force required to pull the wire through the drawing die has historically been a mystery and as Leonardo da Vinci wrote "The amount of force necessary to draw wire through a draw plate cannot be known except through experience" [8]. During the 1900's the force requirement was investigated by several research groups, Siebel and Kobitzsch derived an equation for the drawing force [42]. Wistreich performed parallel studies and came up with a similar equation [40]. Avitzur also derived an equation for the drawing force similar to the previous researchers [47]–[49].

One of the most well-known ways to calculate the drawing force in a wire drawing process is to use the equation derived by Seibel and Kobitszh [42]. The equation for the total drawing force (F) is divided into three parts: homogenous deformation (F_h), inhomogeneous deformation (F_{ih}) and friction during deformation (F_f):

$$F_h = A_1 R_{em} ln \frac{A_0}{A_1} \quad (4)$$

$$F_{ih} = A_1 R_{em} \frac{2\alpha}{3} \quad (5)$$

$$F_f = A_1 R_{em} \frac{\mu}{\alpha} ln \frac{A_0}{A_1} \quad (6)$$

By adding Equation (4)-(6) the total drawing force (F) can be obtained

$$F = A_1 R_{em} \left(ln \frac{A_0}{A_1} + \frac{2\alpha}{3} + \frac{\mu}{\alpha} ln \frac{A_0}{A_1} \right), \quad (7)$$

where R_{em} is the mean yield stress of the wire material before and after the draw, 2α is the die angle and μ is the coefficient of friction.

The equation adds the forces that occurs in the deformation zone (the conical part), however, there is no part added for the bearing area. This is based on the assumption that there is no contact between the wire and the die in the calibration part (bearing zone) of the die, which could be considered as rather doubtful. Persson and Enghag thought so as well, leading to their further development of Equation (7) and adding a part for the frictional force in generated in the bearing [50]

$$F_{fb} = \pi d_1 B R_{e1} \mu \,, \quad (8)$$

where d_1 is the diameter of the reduced wire, B is the bearing length in millimetre and R_{e1} is the yield stress of the reduced wire. Adding this to Equation (7) results in

$$F = A_1 R_{em} \left(ln \frac{A_0}{A_1} + \frac{2\alpha}{3} + \frac{\mu}{\alpha} ln \frac{A_0}{A_1} \right) + \pi d_1 B R_{e1} \mu \ . \ (9)$$

Avitzur [47] also had an idea how to include the bearing length in the calculation of the drawing force but excluded the term in a later publication [48]. Avitzur had a similar approach to calculate the drawing force as Siebel and Kobitzsch, with an equation built on three components which together contribute to the total drawing force, Internal – power term (W_i), Shear – loss term (W_s) and Friction – loss term (W_f).

$$W_i = 2\, f(\alpha) ln \frac{R_0}{R_f}, \ (10)$$

where R_0 and R_f are the radius of the drawn wire before and after the reduction and

$$f(\alpha) = \frac{1}{sin^2 \alpha} \left(1 - cos\ \alpha \sqrt{1 - \frac{11}{12} sin^2 \alpha} + \frac{1}{\sqrt{11 * 12}} ln \frac{1 + \sqrt{\frac{11}{12}}}{\sqrt{\frac{11}{12}} cos\ \alpha + \sqrt{1 - \frac{11}{12} sin^2 \alpha}} \right) . \ (11)$$

Further,

$$W_s = \frac{2}{\sqrt{3}} \left(\frac{\alpha}{sin^2 \alpha} - cot\ \alpha \right) \quad (12)$$

and

$$W_f = \frac{2}{\sqrt{3}}\, \mu \left(cot\ \alpha\, ln \frac{R_0}{R_f} + \frac{B}{R_f} \right) . \ (13)$$

By combining the Equations (10), (12) and (13) an equation for the drawing force including the bearing is obtained,

$$F = A_1 R_{em}\left(2\,f(\alpha) ln\frac{R_0}{R_f} + \frac{2}{\sqrt{3}}\left(\frac{\alpha}{sin^2\alpha} - cot\,\alpha\right) + \frac{2}{\sqrt{3}}\,\mu\left(cot\,\alpha\, ln\frac{R_0}{R_f} + \frac{B}{R_f}\right)\right). \quad (14)$$

However, Avitzur [48] subsequently simplified the equation , $f(\alpha)$ was approximated to 1, the term for shear loss was simplified to, $\frac{4}{3\sqrt{3}} tan\,\alpha$, and the part for the frictional loss in the bearing was removed from the term for friction loss, resulting in,

$$F = A_1 R_{em}\left(2\,ln\frac{R_0}{R_f} + \frac{4}{3\sqrt{3}} tan\,\alpha + \frac{2}{\sqrt{3}}\,\mu\, cot\,\alpha\, ln\frac{R_0}{R_f}\right). \quad (15)$$

Looking at the presented equations used to estimate the drawing force it is found that all parameters except one can be obtained by measuring the geometrical properties of the drawing die and the material properties of the drawn wire. However, one parameter is still unknown and this is the coefficient of friction, which is the parameter that explain how well the process is working. The wear rate of the drawing die is also highly dependent on the friction between the wire and the drawing die. A higher friction will increase the abrasive wear of the die. Friction coefficients for a well-functioning dry drawing process can be found in the literature. Values in the range of 0.01 – 0.07 for a dry drawing process and between 0.08-0.15 for a wet drawing process are to be considered as normal [36], [51]. The friction coefficient can be extracted from the any of the presented drawing force equations, as an example this has been done for Equation (7) resulting in

$$\mu = \alpha\frac{F - A_1 R_{em}\left(ln\frac{A_0}{A_1} + \frac{2\alpha}{3}\right)}{A_1 R_{em} ln\frac{A_0}{A_1}}. \quad (16)$$

By using such an equation combined with drawing force measurements it is possible to achieve a measurement the performance of the lubrication in a specific process. Industrial drawing machines used for normal production are seldom equipped with equipment for measuring the drawing force. However, some modern wire drawing machines have the possibility to read the torque from the motors which rotate the capstan pulling the wire

through the die. This torque has not yet been proven to be useful for this type of measurement, this is probably because there are normally several transmission steps between the motor and the actual pulling of the wire. It is common to have a gearbox and a belt transmission between the motor and the capstan, which will add speed dependent noise to the measurements.

3.2 Temperatures

As explained in chapter 2.2 the temperatures occurring in the drawing process are of high importance for productivity since it affects the performance of the lubricant. As the temperature is dependent on the production rate, it is an important factor to understand and to keep in mind when trying to increase the productivity. As the lubrication efficiency deteriorates, *F* will further increase due to the increase in the coefficient of friction between the wire and the drawing die, leading to even more increase in temperature.

3.2.1 Wire temperature

One research study with FEM-analysis, led to the development of an equation that can be used to estimate the increase of temperature which occurs during one reduction step in a wire drawing process [52].

$$\Delta T = k\frac{F/A_1}{\rho C_p}, \quad (17)$$

Where ΔT is the temperature increase, ρ is the density of the wire, C_p is the wire materials specific heat capacity and k is a correction factor. The loss of energy from the wire that the constant k represents is mostly due to the cooling of the wire in the drawing die. This in turn depends on the design of the die cooling system and the thermal conductivity of the wire and die material [36]. About 0-15 % of the energy that is added to the wire during the reduction is removed due to the cooling in the drawing die [36], [53]. For the process to work in an efficient way the remaining added energy needs to be removed from the wire before the wire enters the next reduction step. This is normally done by adding many turns of wire on the capstan which

pulls the wire. Cooling is added internally in the capstan and the heat is thereby removed from the wire through the capstan to the coolant. However, as the production rates are increased this cooling might not be sufficient to bring the wire back to the original temperature. This will cause heat to accumulate in the wire causing the wire temperature to increase for each drawing step, a schematic example is shown in *Figure 3.1*.

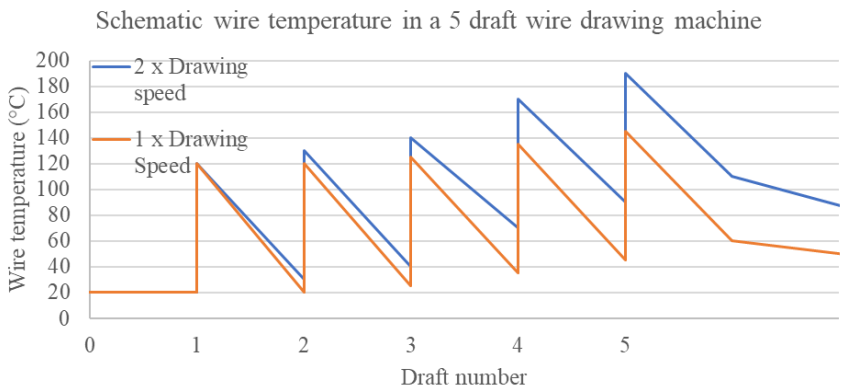

Figure 3.1. Schematic figure showing the temperature increase in the wire caused by an increase in production rate combined with insufficient cooling.

3.2.2 Wire – Die surface contact temperature

In the contact region between the wire and the die the temperature is higher, this due to the frictional force between the wire and the drawing die, this temperature can be estimated using an equation derived by Whright [54]

$$\Delta T_f = \tau_L \sqrt{\frac{Vz}{c_p \lambda}}, \quad (18)$$

where τ_L is the shear stress of the lubrication film, z is the contact length between the die and the wire and λ is the heat transfer rate of the wire.

3.2.3 Die temperature

The temperature of the drawing die affects the hardness of the die material, which influences the wear rate of the die [55]. The cemented carbide used for the drawing dies has around half of its strength at 800˚C [56]. Simulations of the wire drawing process have shown temperatures exceeding this temperature [23], [55].

As explained by the Equation (17), a larger drawing force will increase the heat generated in the forming process and as it is a percentage of the total heat which ends up in the drawing die, this will also lead to an increase in die temperature, affecting the performance of the lubricant, the lifetime of the die and thereby the efficiency of the process.

Also, as for the wire temperature, there will be an increase in die temperature when increasing the production rate. Even if the wire is sufficiently cooled, the die temperature will increase due to the fact that the cooling parameters are constant but there is a need to remove more heat per time unit, since

$$P = F * V \quad (19)$$

and

$$P_{die} = P * k \quad (20)$$

further

$$Q = P_{die} \, . \quad (21)$$

Where P is the power needed for the reduction of the wire, V is the production rate in m/s, P_{die} is the energy that is going to the drawing die and Q is the heat being removed from the drawing die. As can be seen, if the production rate is increased, Q must also increase to obtain an energy balance. As the heat is being transported from the die to the coolant, there are several materials and transfers for the heat to pass through. This means that Q can be defined as the smallest of these values representing each transport through a material and each transfer between the materials,

$$Q = min \begin{cases} Q_{DieHolder-Coolant} = \alpha_C A_{DH} \Delta T_{DH-C} \\ Q_{DieHolder} = \kappa_{DH} \Delta T_{DH} G_{DH} \\ Q_{Die-DieHolder} = \alpha_{D-DH} A_D \Delta T_{D-DH} \\ Q_{Die} = \kappa_D \Delta T_D G_D \end{cases} \quad (22)$$

where α is the heat transfer factors, A is the contact areas, ΔT is the temperature differences, G is a geometry factor and K is the thermal conductivities. Looking at the equations representing Q, it can be seen that if the system parameters are considered to be constant, meaning the temperature of the coolant, the heat transfer factors, the geometry of the drawing die and the thermal conductivity of the used materials, there is only one parameter that can change to compensate for the required increase of Q: the temperature difference. However, as we considered the temperature of the coolant to be constant, it is the temperature of the drawing die that must increase to achieve a higher Q, this explains why the temperature of the drawing die increases with an increased production rate and why it is very important to keep temperature in mind when trying to increase the productivity of the wire drawing process.

4 Process problems affecting productivity and sustainability

This chapter will present common problems that occur in an industrial wire drawing process.

Problems such as surface defects, high tool wear rate and wire breaks are commonly found in industrial wire drawing processes. These types of problems often occur due to problems with the lubrication. If the efficiency of the lubrication is for some reason changed, this leads to a temperature increase, as explained in chapter 3.2, which further affect the lubrication efficiency, explained in chapter 2.2. Failure to correct the problem can result in damage to the tool and the produced wire.

4.1 Increased tool wear

Tool wear is highly dependent on the effectiveness of the lubrication, i.e. the friction between the wire and the die, as explained in chapter 2.1.1. According to Equation (1) the tool wear is dependent on the constant k_f which represents the friction in the system. The wear is also dependent on the drawing force, which according to Equation (7) is also dependent on the friction coefficient of the wire-die system. Furthermore, as explained in Chapter 3.2.1, the temperature of the drawing die is related to the drawing force, and as shown in a previous study, the die wear rate is dependent on this temperature [55]. As there is a constant H in Equation (1) which represents the hardness of the die material which is dependent on the temperature of the drawing die [56] this is not a surprise.

This means that it is very important to choose the right lubricant for the specific process, so that the temperature in the process lies within the optimal temperature span of the chosen lubricant [36], [45], [46]. Running a process without optimizing the lubrication will cause an increase in the tool wear, leading to decreased time between tool changes, leading to decreased productivity and sustainability. This is also something that might be exceedingly difficult to detect since in many cases the drawing dies are changed a long time before they are

worn-out due to the production planning. By assuring a well-functioning lubrication process at all times the tool wear can be kept at minimized pace.

4.2 Surface defects and wire breaks due to poor lubrication

Even if a suitable lubricant has been chosen for the specific process there are a lot of different factors that can create problems with the lubrication, these problems include running out of lubricant, tunnels in the lubricant, moisture, caking, blockages of the die entrance and cooling problems [36], [51]. *Figure 4.1* shows an example of blockage at the die entrance due to insufficient cooling of the drawing die resulting in lubricant being pushed back instead of following the wire through the die, preventing fresh lubricant from entering the die.

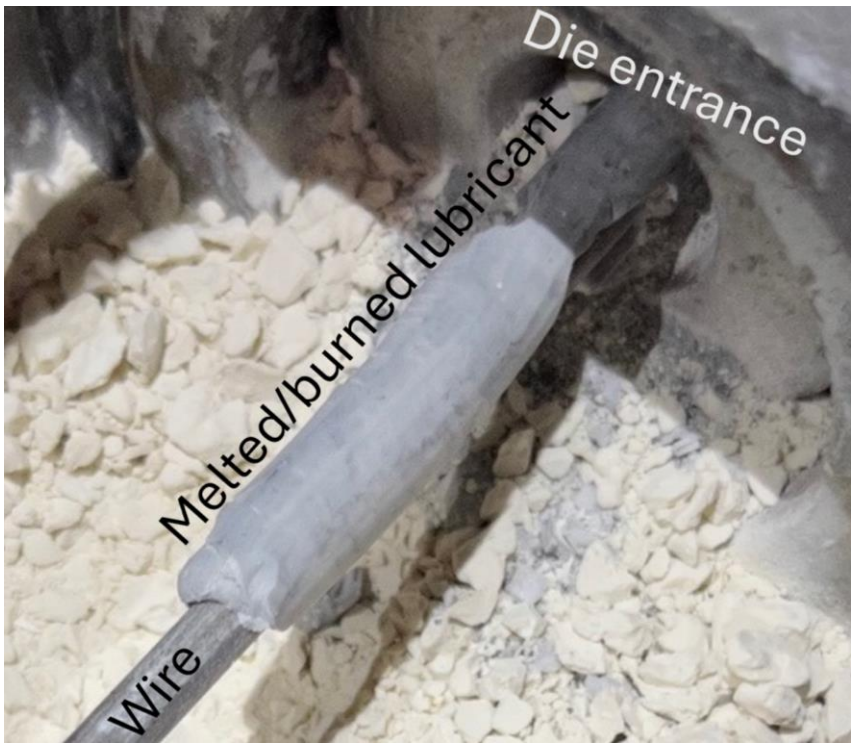

Figure 4. 1. Blockage in form of a pipe consisting of melted/burned lubricant at die entrance preventing fresh lubricant from entering the drawing die.

Lack of lubrication leads to metallic contact between the wire and the die which can lead to galling, a kind of severe adhesive wear [57], [58]. Material from the wire can be transferred to the die surface, with the result that the added wire material scratches the wire as it passes through. This is one of the most difficult problems to detect, since the scratches can be microscopic and still be critical. Also, the scratch might not be found on the whole produced spool of wire, it will start at a certain point, and it can actually heal itself, if the material which is welded to the die comes loose. This makes this defect very difficult to find.

If the process is allowed to continue running, the efficiency of the lubricant might further degrade, and this will lead to more metallic contact between the wire and the die. The brightness of the wire surface might change as the lubricant is no longer present at the wire surface.

If allowed to run even further, the temperature increase might lead to total breakdown of the lubrication, at this point the wire often becomes very bright as there is no lubricant on the wire surface, instead there is fresh steel material exposed. Finally, a wire break will probably occur due to the high friction. *Figure 4.2* shows these steps starting with a wire produced with a well-functioning lubrication process.

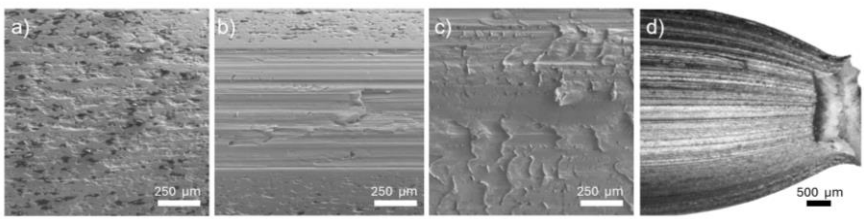

Figure 4.2. a) Wire produced with well-functioning lubrication b) a scratch on the wire surface c) very rough surface due to poor lubrication d) wire break due to no lubrication (SEM images (a-c) from Paper III)

5 Monitoring of the wire drawing process

In many industries monitoring of certain process-sensitive parameters is common to ensure that a process works as it should. By monitoring these parameters, it can be ensured that the process is functioning as intended. However, in wire drawing, process monitoring is still not yet implemented by the industry. Monitoring of the wire drawing process has been studied by many researchers during a long period of time, but still the industry standard is that the operator visually inspects the wire.

This chapter presents a literature review of the previous work in the field of wire drawing process monitoring. Methods that will be developed and investigated in this thesis are also presented and described in depth.

5.1 Previous work

The possibilities of monitoring the wire drawing process have been explored by researchers for the last four decades. The focus has been on trying to evaluate lubrication performance in-situ as the lubrication is the most vital factor for the wire drawing process to work. Several different approaches have been made using vastly different techniques.

5.1.1 Resistance between die and wire

A Swedish research group led by Bruno Nilsson worked over twenty years (1980-2001) with developing a method and a device that measured the electrical resistance between the wire and the die [59]–[63]. The researchers claimed that resistance would indicate the status of the lubrication performance in the wire drawing process. If the lubrication layer thickness between the wire and the die changed, the resistance between them would also change. Thus, poor lubrication would result in low resistance. The researchers also tried to correlate the resistance value to the actual amount of residual lubricant on the wire surface. Nilsson also developed an industrial process monitoring system using their method, which was called the “Tearing detector”,

the product was sold in a small number at the time when it was released [64].

5.1.2 Vibration measurement

Vibration measurement is a technique that have been evaluated by several research groups and companies for monitoring the wire drawing process, with good results over the last four decades. In 1984 a patent for flaw detection in wire drawing using acoustic emission was filed. This was inspired by a paper published in 1980 about assessment of the frictional condition in wire drawing using acoustic emission [65], [66]. During the 1980's several attempts were made using acoustic emission for monitoring the lubrication process in wire drawing [67], [68]. In the beginning of the 2000's the same Swedish research group mentioned in section 5.1.1 used acoustic emission and came to the conclusion that the information from the measurement could contribute to several monitoring purposes [63]. In 2018 acoustic emission was used by a company that developed a process monitoring tool for wire drawing leading to a patent and a product [69]. However, to the author's knowledge the implementation of the system in the wire drawing industry has been very limited. More recently a research group has again used acoustic emission to try to monitor the wire drawing process. The findings from their studies are interesting since they find that by using acoustic emission it is possible to detect which type of lubricant that is used and also they find a high correlation between the acoustic emission and the tool temperature [70], [71].

Common for all these attempts is that they have used acoustic emission to collect the vibration data from the wire drawing process.

5.1.3 Temperature related measurements

In 2001 Nilsson performed pre-studies on different ways to monitor the drawing process using indirect measurements [63]. Two investigated methods suggested were related to process temperature namely, the thermoelectric voltage occurring between core and case of the drawing die and the thermoelectric voltage occurring between

core and wire. He found that both had potential and that further studies should be conducted.

In 2014 an investigation of possible monitoring processes for the detection of defects in the wire during the wire drawing process was made by the author of this thesis. One of the methods that was investigated was the use of a pyrometer to monitor the wire drawing process as the wire was wound on the block in the drawing machine. Experiments showed promising results in detecting complete loss of lubrication. However, when using a pyrometer there is a disadvantage, the exact position and size of the measuring point is unknown. At the distance which the pyrometer was mounted from the block the measuring point was larger than the diameter of the wire. This resulted in problems when the wire was unevenly wound on the block, the pyrometer would measure the temperature of the block instead of the wire, see *Figure 5.3* [72].

5.2 Investigated monitoring methods

In this thesis three different methods to monitor the wire drawing process are developed and evaluated, these are:

- Vibration measurement
- Wire temperature measurement
- Wire brightness measurement

These three methods were chosen because of the following reasons.

Vibration measurements in the form of acoustic emission have, as mentioned in section 5.1.2, been evaluated, and proven to be a good parameter for process monitoring several times during the last 40 years. However, even though it has been proven to work, there has not been any implementation of such systems in the wire drawing industry. This indicates that there might be an issue with the acoustic emission measurements in an industrial environment, but in view of the promising results it is nevertheless an interesting method. However, there are other ways to measure vibrations which have been evaluated in this thesis.

Wire temperature is, as explained in section 3.2, directly related to the drawing force which has previously proven to be a good indicator of the process status. Wire temperature has great potential to be used for monitoring since it is dependent on the drawing force and it should be rather easy to implement measurement.

The brightness of the wire surface is the most common way which is used by the machine operators today to check the status of the process. An experienced operator can assess much from just looking at the wire as it is wound to the capstan. However, the machine operator is not standing by the machine all the time, normally one operator runs several machines. Also, the work force is changing faster in today's society and to become an experienced operator takes time, often several years. As the brightness of the wire is the method which is commonly used in the industry today it should have great potential to be used for process monitoring.

5.2.1 Vibration measurement

As described in section 5.1.2, there have been several attempts to use acoustic emission for monitoring the wire drawing process. However, the method has not been successfully implemented in the industry, even though, investigations have been made since the 1980's. This leads to the assumption that the method is not suitable for industrial use. However, the research studies performed over the years which have used acoustic emission measurements have shown promising results, that the acoustic emission measurements give vital information about the status of the wire drawing process.

Another method that could be used to measure vibrations is by means of an accelerometer. In the past, accelerometers have been very expensive, but since the introduction of accelerometers without moving parts, the low price have made them much more available. Today accelerometers can be found in vastly different applications - for example in every smartphone. Using an accelerometer have the potential to be less sensitive to disturbances not related to the drawing process, this because the method measures the movement of the sensor instead of sound, meaning that ambient noises, for

example if an operator drops a tool on the floor making a loud noise, will not be registered as a problem in the process.

5.2.1.1 Development of method to measure and analyze vibrations in the wire drawing process

To measure vibrations in the wire drawing process a sensor was needed to sample the vibrations created as the wire is drawn. Today there are many industrial solutions that can be used out of the box, but when these studies started (2012) it was still quite expensive and not that common. For this type of initial work, it is very important to be able to ensure full control over the measurements, so it is necessary to verify that the raw data is captured and that no filtering is made. For these reasons, a simple sensor was designed for the specific purpose. The sensor was based on a ADXL 335 chip bought on a simple breakout board. The circuit was modified to get the full frequency range of the accelerometer chip, the board with the sensor is shown in *Figure 5.1*.

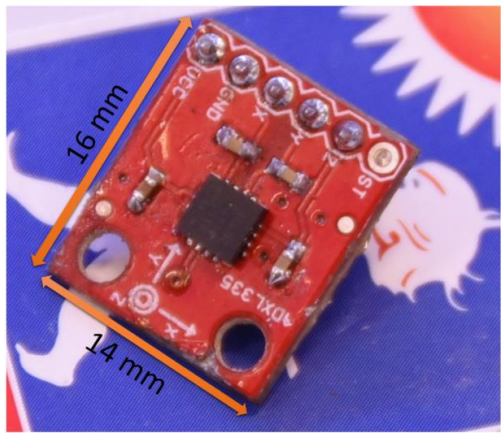

Figure 5.1. Accelerometer board used for making the vibration sensor.

The accelerometer chip supplies an analog signal representing the current g-force, this signal was sampled at 12500 Hz using a DT9600 which is an analog to digital data acquisition tool for use with a normal computer with an USB-port.

To get understanding of the captured signal, Fourier transformations were made on signals representing different stages of a drawing process. Also, vibration data not only from the drawing direction but from x, y and z were captured and kept in the analysis.

The hypothesis is that the captured vibration signal will indicate changes in the lubrication performance in a similar manner as the drawing force signal, meaning that poor lubrication should generate higher amplitude in the captured signal.

5.2.2 Wire temperature measurement

As presented in chapter 2.2 and 3.2, the temperature is of highest importance for the functionality of the lubrication process. Also as presented in Equation (17), the wire temperature is dependent on the drawing force, meaning that by means of wire temperature measurement the drawing force can indirectly be measured. The temperature of the drawn wire can be measured in several different ways, these different methods can be categorized into tactile and optical measurements. Both types of measurements have their pros and cons. Tactile temperature measurement of the temperature on the wire surface can be performed by using a riding thermocouple, which is a small wagon with wheels riding on the wire, in between the wheels there will be a spring-loaded thermocouple measuring the temperature of the wire surface. This works for most wire materials, but for some materials which are close to the thermocouple in the triboelectric series, large measurement errors will occur. Also, in most high-quality wire production processes all unnecessary contact with the wire should be avoided. A riding thermocouple is shown in *Figure 5.2*.

Figure 5.2. Riding thermocouple for measuring wire temperature.

Optical methods to measure the temperature of the drawn wire includes IR-pyrometry and thermal imaging. However, both methods are sensitive to the brightness of the wire surface affecting the emissivity. The emissivity might in some cases change as the lubrication state changes, meaning that the measured temperature might change even though the actual temperature is still constant. In the work included in this thesis, optical methods have been used to measure the temperature of the wire.

5.2.2.1 Development of method to use the temperature of the drawn wire for in-situ measurement of lubrication performance

As previously stated, the temperature is dependent on the drawing force, meaning that a change in the drawing force should be measurable on the wire temperature. Examining Siebel's equation for drawing force, Equation (7), it can be seen that a change in drawing force, if the wire material and drawing die are unchanged, must come from a change in friction coefficient. A change in the friction coefficient means a change in the performance of the lubrication system. The drawing force equation has been rearranged to be able to calculate this friction coefficient, Equation (16). Further, looking at Equation (17), the equation to estimate the temperature of the drawn wire, it can be seen that all the constituent parts except the drawing

force can be considered as constants if the same assumption is made as for the drawing force equation, i.e. that the material properties of the wire do not change. However, there are some uncertainties regarding the loss constant that need to be measured for the specific process. By combining these two equations (16 and 17) it is possible to get an equation for estimating the performance of the lubrication system by using the wire temperature,

$$\mu = \frac{\alpha \Delta T \rho C_p}{ln\frac{A_0}{A_1} K R_{em}} - \alpha - \frac{2\alpha^2}{3ln\frac{A_0}{A_1}}. \quad (23)$$

The hypothesis is that μ calculated using the measured temperature (Equation (23)) will change in the same manner as μ calculated using the drawing force (Equation (16)), indicating on the lubrication performance of the process.

5.2.2.2 Development of thermal imaging method

As mentioned, previous in chapter 5.2.2, there may be difficulties measuring the temperature of the wire surface using optical methods, due to the changing emissivity of the wire surface. The purpose of the development of this method was to achieve a monitoring method which can be used without knowledge of the emissivity of the drawn wire or any other material parameters. The hypothesis set is that if the lubrication conditions of the wire drawing process change, then the signal from the thermal imaging camera will also change. This change is depending on three process factors;

- The temperature of the wire, as explained in the previous chapter.
- The emissivity of the wire surface, there is a significant difference in the reflectivity between an unlubricated and a lubricated wire surface, as explained in chapter 5.2.3.
- Damage on the wire surface, patterns in the thermal images caused by both changes in temperature and emissivity.

Instead of looking at the absolute temperature value of the wire surface, the idea is to look at differences in measured temperature

over the wire surface. This can be done by using the pixel value distribution over a small area of the wire surface. The pixel value standard deviation (σ), will be defined as,

$$\sigma = \sqrt{\frac{1}{N}\sum_{i=1}^{N}(x_i - \gamma)^2}, \quad (24)$$

where x_i is the value of one pixel and,

$$\gamma = \frac{1}{n}\sum_{i=1}^{n} x_i \, . \quad (25)$$

Further filtering of the monitoring signal is done by applying a calculation of the maximum standard deviation for each second,

$$T_s = Max_{i=1}^{F_R}\, \sigma_i \, , (26)$$

where T_s is the thermal imaging monitoring signal and F_R is the frame rate with which the thermal images are captured.

The hypothesis is that σ will change as the status of the wire drawing changes.

5.2.3 Wire brightness measurement

The brightness of the wire is used today by the operators using visual assessment. As stated in section 5.2, it takes long time to train a new operator to learn to spot the differences in the color of the wire and how to control the process depending on what is observed. Also, when running many different products, it can be tricky to remember the differences in surface brightness between them, what might be considered good for one product might not work for another. The machine operator does not stand by the drawing machine looking at the wire at all times. When the machine is started, and everything looks good the operator has to continue the work at other machines and so on. Monitoring the brightness with cameras makes it possible to continually look at the wire brightness. *Figure 5.3* show an example of wire being produced with an unstable lubrication process.

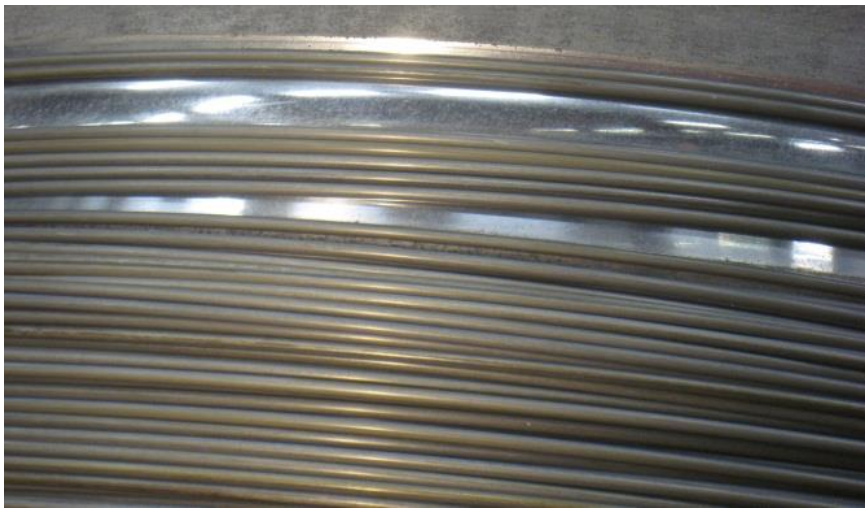

Figure 5.3. Drawn wire on a capstan, note the color differences on the wire turns, indicating on an unstable lubrication process.

5.2.3.1 Development of a method to measure and analyze the brightness of drawn wire in-line

The idea of the method is to use a camera that continuously capture images of the wire surfaces and then analyses the brightness of each captured image. To be able to perform such measurements a sensor was designed utilizing a CCD-sensor, in this case an 8-bit webcam running at a resolution of 640x480 pixels. For the method to be stable and not dependent on the surroundings, the images of the wire need to be taken in a protected environment. This environment was achieved by designing a special camera housing which is shown in Figure 5.4. The sensor was designed as a splitable pipe with hinges, this allows for an easy changeover procedure when the wire needs to be changed. The dimensions of the pipe section of the housing were ∅10 *mm* internally and 150 *mm* in length.

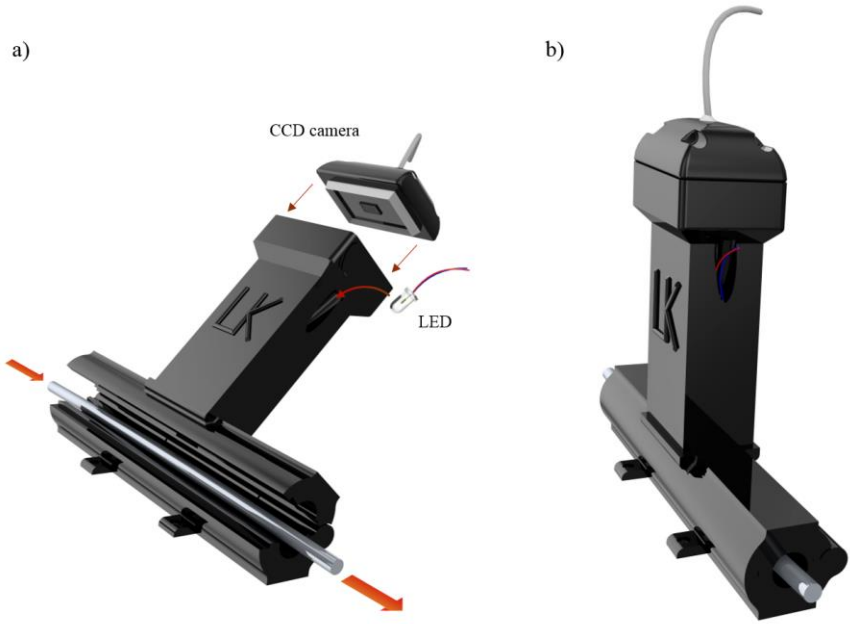

Figure 5.4. a) Rendering of the open sensor housing, displaying the wire drawing direction, the placement of the CCD-camera and the LED b) Closed housing (Figure from Paper IV)

The housing was fabricated in black colored plastic (polylactide) by means of fused filament fabrication. The CCD-camera was placed on top of a duct looking down on the wire. The duct also contained a white LED with a 30° beam angle that illuminated the wire. The length on the CCD-camera duct was adapted to focus the camera on the wire surface. The view that the CCD-camera had of the wire can be seen in *Figure 5.5a.*

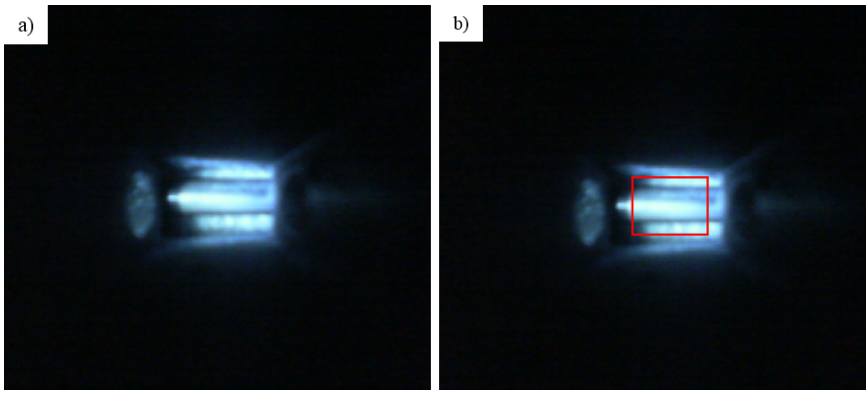

Figure 5.5. a) The wire as seen by the mounted CCD-camera b) The red rectangle encloses the pixels used to calculate an average reflection intensity. (Figure from Paper IV)

The brightness of every image was calculated by looking at intensity of the reflection caused by the LEDs illumination of the wire. To get a comparable measurement, the average intensity in the region of interest seen in *Figure 5.5b* was calculated. The average intensity was calculated from these 30x70 pixels by using the following expression,

$$I_A = \frac{\sum_i^{N_R} \sum_j^{C} I_{i,j}}{N_R \cdot C}, \quad (27)$$

where I_A is the average intensity of one frame, N_R the row of pixels, C the columns of pixels, and $I_{i,j}$ is the intensity of a pixel in position i and j.

The hypothesis is that I_A which represents the brightness of the wire will change as the performance of the lubrication changes.

6 Results and discussion

In this chapter, the results from the performed investigations will be presented and discussed. The focus of the investigations is to study if the proposed monitoring methods can indicate changes in process performance and the characteristics of the drawn wire.

6.1 Investigation of theoretical methods to evaluate the friction coefficient

The method to calculate the coefficient of friction is a central part of being able to estimate the performance of the lubrication process. The following investigation was conducted in Paper I to compare the different methods to estimate the friction coefficient from measured drawing force. As described in section 3.1, there are several methods to calculate the required force to pull the wire through the drawing die. This study was performed to investigate which of the available drawing force theories generates results that are consistent and reflect the real process. Another outcome of the study was a novel equation for predicting the drawing force, see Paper I.

To generate data that could be used to compare the different methods for calculating the drawing force, a set of wire drawing experiments were designed where the only parameter that was changed in between the experiments were the length of the cylindrical part of the die, the bearing. This part of the die was chosen as the variable since this part is included in some of the drawing force equations but left out in others.

The hypothesis is that the coefficient of friction for the die-wire system should not change with the bearing length. The bearing part of the die probably has a rather small impact on the drawing force, and if the friction coefficient of the complete wire-die system is changed due to the change in bearing length it is considered to be incorrect. Also, the calculated coefficients of friction from the different equations are used as input for finite element models that are used to calculate the drawing force. The drawing force values from the finite element analysis are then compared to the drawing

forces measured during the experiments, this is done to evaluate the accuracy of the different drawing force equations.

The experiments were performed at the wire drawing laboratory at Örebro university, in the single capstan wire drawing machine. During each experiment approximately 30 m of wire was drawn. The drawing dies used for the experiments are presented in *Table 6.1*.

Table 6. 1. Geometrical parameters for the drawing dies used in the experiments. The bearing is expressed in length (mm) and as a percentage of the die diameter. (Table from Paper I)

Drawing die	Diameter (mm)	Die angle (°)	Bearing length (mm)	Bearing (%)
1	3.80	12.2	0.35	9.3
2	3.81	12.3	0.85	22.4
3	3.80	12.2	1.28	33.8
4	3.81	11.7	1.64	43.2
5	3.80	12.0	2.30	60.7

During the experiments the drawing force was measured using two force sensors that were fitted to the drawing box in such a way that all the force required to pull the wire was lead through the sensors. The force sensors used for this were of KIS-2 type and had a range of 0-30 kN with an error of < 1 %. The signal from the sensors was sampled at 800 Hz and then processed in a *LabVIEW* software, storing mean values measured signal, calculated at 1 Hz.

The evaluated drawing force equations are those presented in chapter 3.2, meaning Equations (7), (9), (14-15). However, to be able to use them to get the corresponding friction coefficient from each experiment the equations needed to be rearranged with respect to the coefficient of friction (this is already done for Equation (7) -> Equation (16)).

$$\mu = \alpha \frac{F - A_1 R_{em}\left(ln\frac{A_0}{A_1} + \frac{2\alpha}{3}\right)}{A_1 R_{em} ln\frac{A_0}{A_1}}. \quad (16)$$

The rest of the equations were rearranged in their corresponding order,

$$\mu = \frac{F - A_1 R_{em}\left(ln\frac{A_0}{A_1} + \frac{2\alpha}{3}\right)}{\frac{A_1 R_{em} ln\frac{A_0}{A_1}}{\alpha} + d_1 \pi R_{e1} B}, \quad (28)$$

$$\mu = \frac{\frac{F}{A_1 R_{em}} - 2\, f(\alpha)\, ln\frac{R_0}{R_f} - \frac{2}{\sqrt{3}}\left(\frac{\alpha}{sin^2\alpha} - cot\,\alpha\right)}{\frac{2}{\sqrt{3}}\left(cot\,\alpha\, ln\frac{R_0}{R_f} + \frac{B}{R_f}\right)} \quad (29)$$

and

$$\mu = \frac{\frac{F}{A_1 R_{em}} - 2\, ln\frac{R_0}{R_f} - \frac{4}{3\sqrt{3}} tan\,\alpha}{\frac{2}{\sqrt{3}} cot\,\alpha\, ln\frac{R_0}{R_f}}. \quad (30)$$

The resulting drawing force from the performed experiments differs by roughly 5% (200 N) between the experiments with the highest and lowest drawing force.

The equations for calculating the coefficient of friction were used on the data from the experiments, resulting in five calculated coefficients of friction for each equation, the result is presented in *Figure 6.1*.

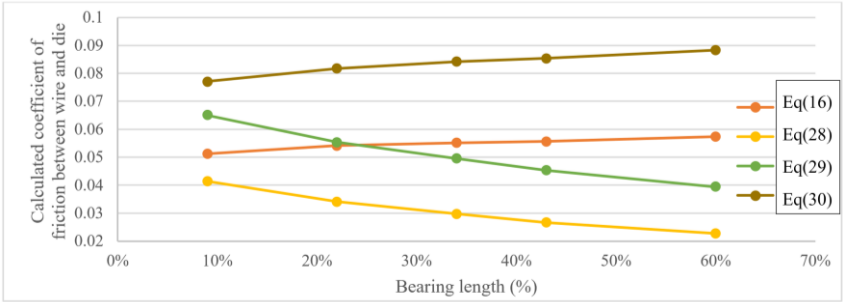

Figure 6.1. Calculated coefficient of friction using the Equation 16 (Siebel), Equation 28 (Persson), Equation 29 (Avitzur with friction bearing) and Equation 30 (Avitzur drawing force equation) depending on bearing length and method.

As can be seen in the results, the equations (28 and 29) which both includes a parameter for the bearing length seems to be overestimating the influence of the friction in the bearing, since the calculated coefficient of friction is decreasing with an increasing bearing length. Equation (30) gives a rather high value for the coefficient of friction for all the performed experiments. As the process was well lubricated it can be assumed that the actual coefficient of friction should be under 0.07 according to the literature [36], [51].

To further evaluate the result from these equations, finite element analyses were performed with the geometrical properties of the drawing dies, the material properties of the used wire and the coefficient of friction calculated using the different equations as input data. The software used for the finite element modeling was Ansys Workbench [73], a coupled thermomechanical axisymmetric model was used for decreased computation time and an implicit solver was used for the calculations. A non-linear material model with bilinear strain hardening was used for the wire material using data acquired from tensile tests. The contact model used was an Augmented Lagrange. An example of a model showing the boundary conditions used is presented in *Figure 6.2*.

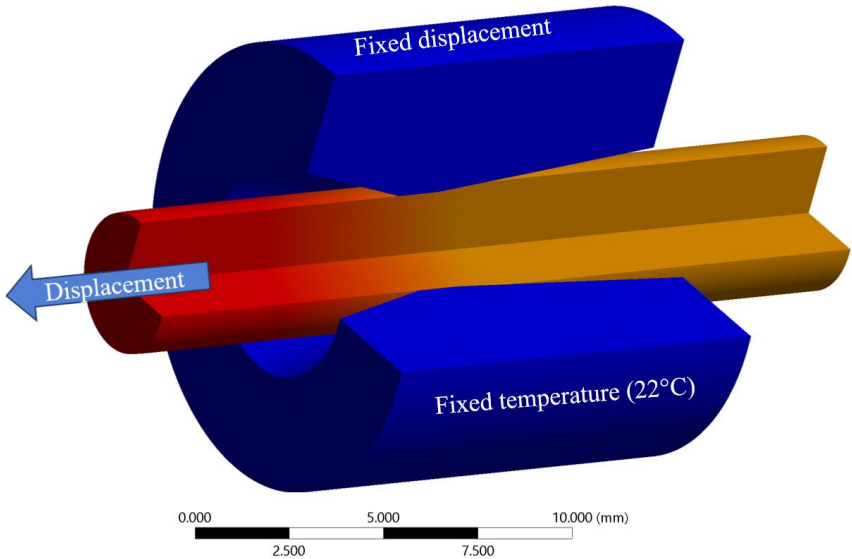

Figure 6.2. Boundary conditions used in the finite element analyses. (Image from Paper I)

The result from the analyses is presented as percentage of difference between the mean drawing force from the simulation and the mean drawing force from the corresponding experiment. The result is shown in *Figure 6.2*, where it can be seen that Equation (16) and (29) gives results closest to reality, under 5% difference for the range of bearing lengths normally used in steel wire drawing (20-40%). However, looking back at *Figure 6.1* it is clear that Equation (29) overestimates the influence of the friction in the bearing part of the drawing die, meaning that the equation will give results further from the real case with an increasing bearing length. The same problem will happen with Equation (16) since it does not include a parameter for the bearing.

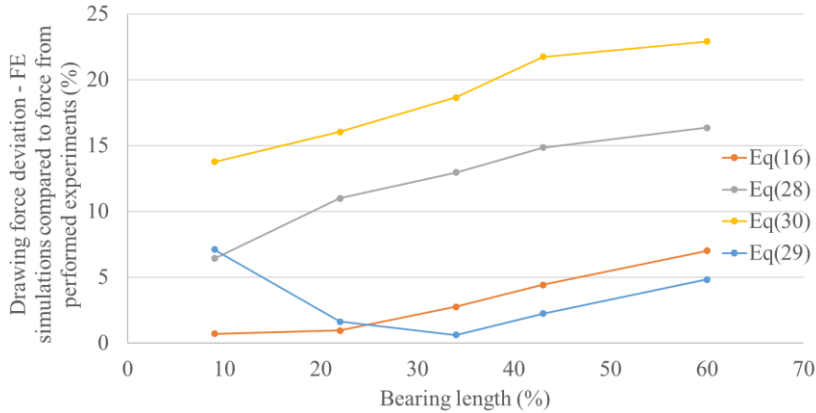

Figure 6.3. Evaluated accuracy of the compared drawing force equations (16) (Siebel), (28) (Persson), (29-30) (Avitzur) comparing finite element results regarding drawing force and the measured mean drawing force from the experiments.

As shown in the results, both Equation (16) and Equation (29) seems to give quite accurate results regarding drawing force/coefficient of friction for drawing dies with normal bearing lengths. However, as Avitzur only presented Equation (29) in the making of Equation (30) it is hardly to be considered to be one of the most common methods to estimate drawing force. Due to this reason the author of this thesis has chosen to use Siebel's drawing force equation in the research studies included in this thesis.

6.2 Vibration measurements

To investigate if vibration measurement by means of an accelerometer is a viable solution for process monitoring of the wire drawing process a set of experiments were conducted and presented in Paper II. The setup used for the experiments to capture the vibration signal and drawing force data is shown in *Figure 6.4*.

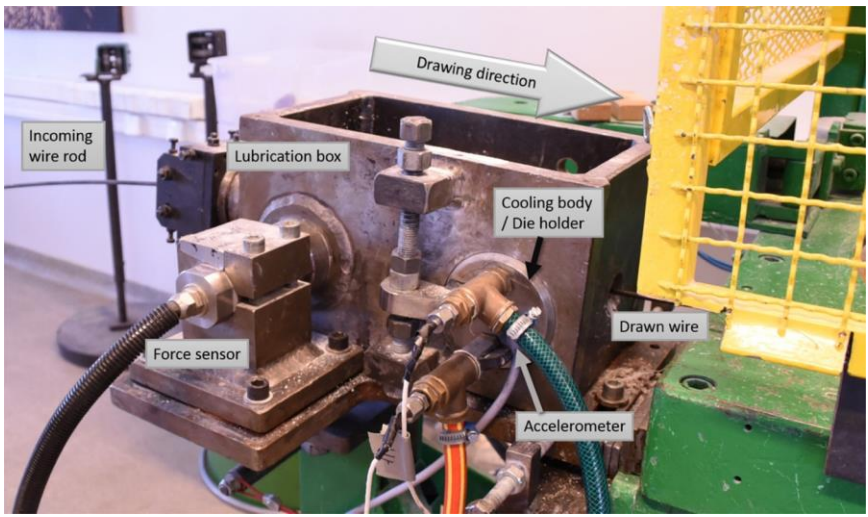

Figure 6.4. Drawing box setup to measure drawing force and vibrations. (Figure from paper II)

Two of the performed experiments to investigate the correlation between the drawing force and the vibration signal were:

- Removal and re-introduction of lubrication during drawing
- Running out of lubricant.

Removal and re-introduction of lubrication during drawing

The experiment was conducted to simulate a sudden loss of lubrication. The lubricant was removed by means of vacuum suction from the drawing box. The resulting signals are presented in *Figure 6.5*, both the investigated signals show a sudden increase. For both of

the signals there is an incubation time during which the higher signals sometimes drop to the previous stable level, this is most likely due to the fact that there is some lubricant still present at the die entrance which for short periods can contribute to favorable lubrication conditions. The process was allowed to run without lubricant for around 60 s, roughly equivalent to 30 m of wire, the lubricant was then added to the process again and this resulted in the reduction of the required drawing force and the vibrations signal also dropped down to the previous stable values. It is thus quite clear that the change in the performance of the lubrication can be detected by both force measurements and by vibration measurements.

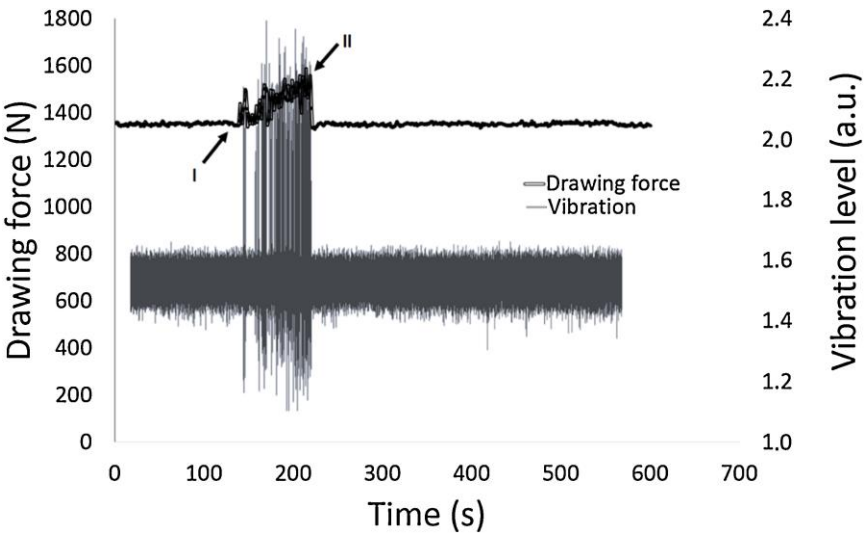

Figure 6.5. Influence of lubrication condition on the measured drawing force and vibration amplitude. The arrows indicate the removal of lubricant (at I) and the reintroduction of lubricant (at II) (Figure from Paper II)

Running out of lubricant

When the lubricant was allowed to run out naturally, the signal pattern is similar to the case of quick removal with the exception that the incubation time, from early indications to constant high vibration/drawing force signals, is longer. The signals are shown in *Figure 6.6*. The lubrication is not as drastically lost as for the case of complete removal of lubricant from the lubrication box and the lubrication situation is thus varying from good to poor for a longer time period. The amount of wire drawn from the first signals of increased vibrations to the end of the experiment is over 100 m in length. The poor lubrication can be detected in both the vibration signal and in the force signal.

Again, it is shown that the loss of efficient lubrication can be detected by both force measurements and by vibration measurements. Also, in this case the results show that the vibration signals give a higher degree of difference between the lubricated and the non-lubricated conditions compared to the use of force signals. The detectability of poor lubrication conditions is thus strongly favored by using vibration signals. Additionally, application of vibration sensors in the wire drawing equipment is much easier than the application of force measurements. In an industrial environment this is of utmost importance. The results also show the importance of early detection of poor processing conditions in order to reduce the amount of material produced with high risk of defects.

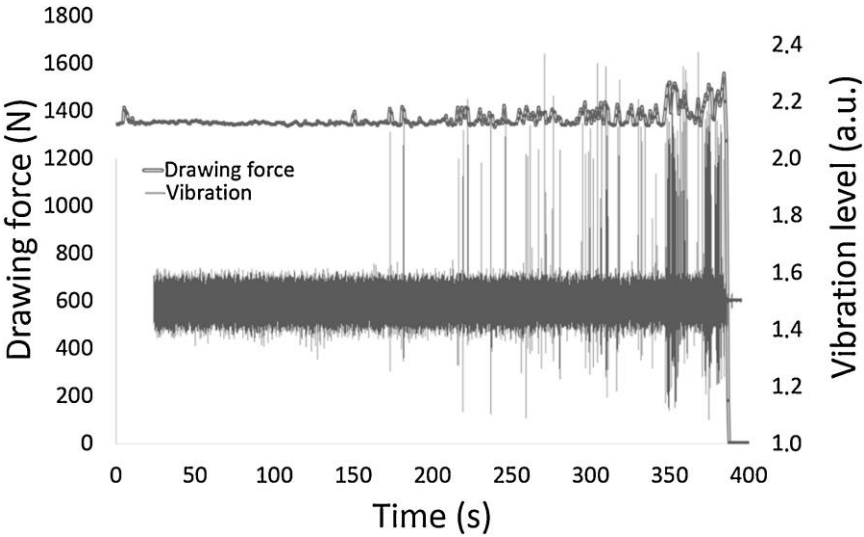

Figure 6.6. Influence of lubrication condition on the measured drawing force and vibration amplitude, as the lubricant is allowed to slowly run out. (Figure from Paper II)

Vibration signal analysis

Most of the events related to change in the lubrication performance captured in the current investigation were detected at the lower end of the frequency domain, under 1000 Hz. *Figures 6.7-6.9* show data from different stages of the experiment presented in *Figure 6.6* that has been treated using Fourier transformation. Consequently, the monitoring of frequencies below 1000 Hz or even lower seems to be conservative enough to capture the important variations in the lubrication performance for process monitoring and control purposes. The largest change in the signal seems to be happening at frequencies below 50 Hz. That is at least for the types of unwanted process conditions that have been investigated in this study.

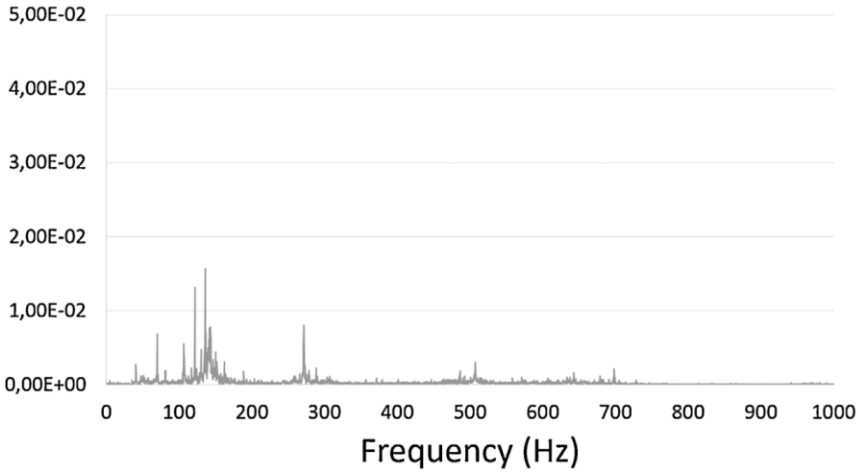

Figure 6.7. Vibration frequencies from the beginning of the experiment where the lubrication was starved when there still was a well-functioning lubrication. (Figure from Paper II)

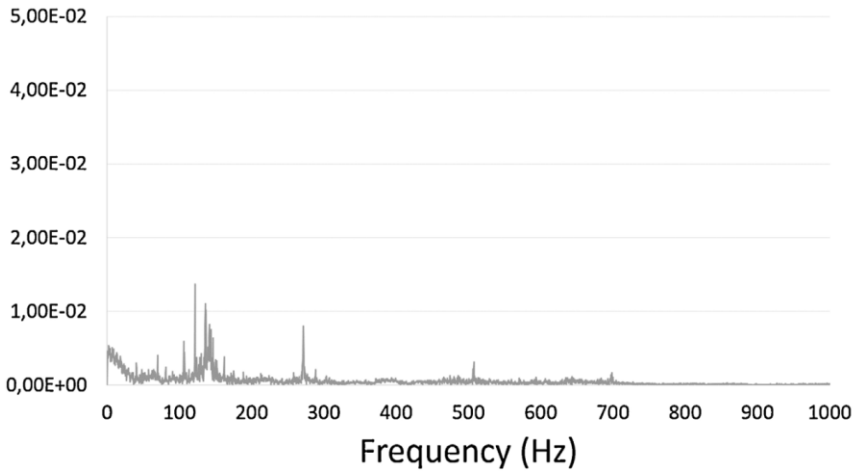

Figure 6.8. Vibration frequencies from the experiment where starved lubrication conditions were reached (corresponding to the appearance of the first two spikes in the vibration signal) (Figure from Paper II)

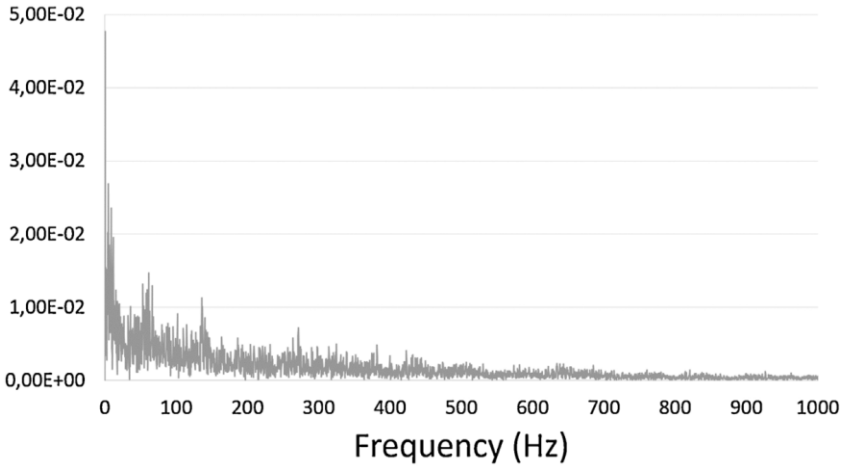

Figure 6.9. Vibration frequencies from the end of the experiment where the lubrication was starved, non-lubricated conditions have been reached (corresponding to the continuously high vibration signal levels) (Figure from Paper II)

These two experiments showed promising results, and in these cases, the unfiltered vibration signal correlated very well with drawing force signal and gave good indications regarding the changes in the lubrication performance in the drawing process.

6.3 Wire temperature measurements

As explained section 5.2.2 the temperature of the wire has a high potential to monitor the performance of the lubrication in the same manner as the drawing force, since according to the theory, the temperature is highly dependent on the drawing force. The studies in Paper III were made to investigate the hypothesis presented under 5.2.2.1 and 5.2.2.2.

To capture thermal imaging data a FLIR A600 series thermal imaging camera was utilized. The camera has a spatial resolution of 0.68 mrad, a field of view of 25° x 19°, a minimum focus distance of 0.25 m, a focal length of 24.6 mm, an IR resolution of 640 x 480 pixels, a detector pitch of 17 μm, thermal sensitivity <0.05 °C at +30°C and a detector time constant that typically is 8 ms. The manufacturer specifies an accuracy of ±2 °C or ±2% of reading [74]. The temperature measurement range used was 0 - 650 °C, the camera was placed approximately 300 mm from the wire, and the image capturing frequency used was 200 Hz. With the chosen image frequency, the camera uses windowing, meaning a subset of the total image is selectively read out. At 200 Hz the camera can handle a window of 640 x 120 pixels. The software that was used to capture the thermal images and later for analyzing the data was ResearchIR from FLIR [75]. The experimental setup used for the trial is shown in *Figure 6.10*.

To provide more understanding of what type of data the thermal imaging camera processes, three examples of thermal images are shown in *Figure 6.11.* These thermal images were captured during different stages of the experiment. Top images shows where the wire drawing process was functioning as intended. Middle image was taken exactly at a point where the wire starts to scratch because a piece of the wire got welded in the drawing die due metallic contact between the wire and the die and the bottom image shows the process producing a wire with a scratch.

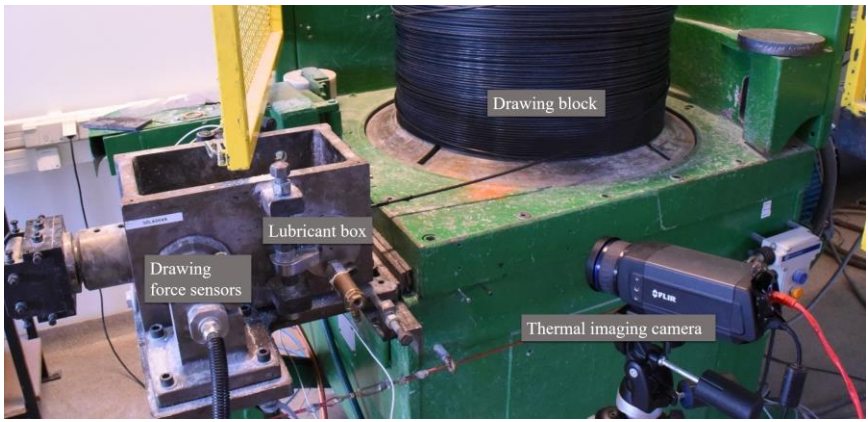

Figure 6.10. Placement of thermal imaging camera, which focuses on the wire as it leaves the drawing box. (Figure from Paper III)

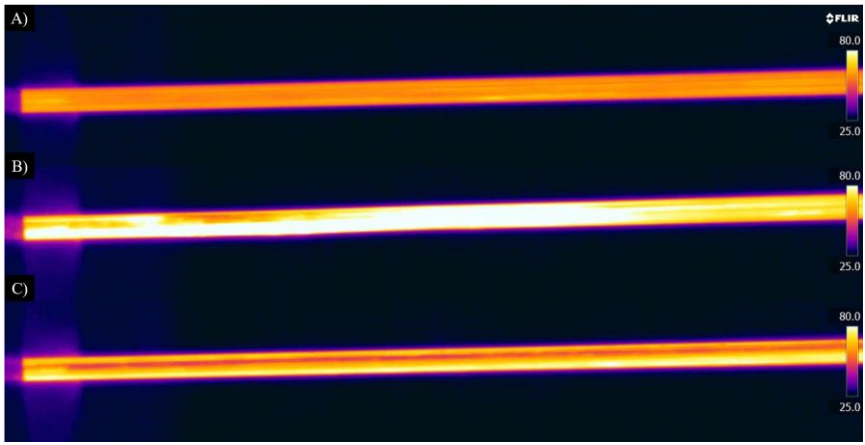

Figure 6.11. Example of thermal images from the experiment. a) Drawing process functioning as intended; b) Picture showing at the exact point where the wire starts to scratch c) unfunctional process producing scratched wire. (Figure from Paper III)

One type of experiment was used to do this evaluation but with two different materials. Only results from one of the experiments will be presented in this chapter, for the other case the reader is referred to Paper III. In the presented study, a stainless-steel grade (X10 CrNi 18-

8 HS) was used. During the experiment, drawing force and thermal images were captured. The experiment was conducted as follows:

- Engage monitoring equipment
- Engage the wire drawing, with lubrication
- Run the lubricated process for approximately 3 min, ensuring that there are stable monitoring signals
- Remove the lubricant from the lubricant box
- Disengage the wire drawing process when the lubrication process has failed (indicated by an increase in the drawing force)
- Disengage the monitoring equipment

Result from the experiments is shown in *Figure 6.12* where the captured drawing force signal is compared to the method presented in chapter 5.2.2.2, the thermal imaging signal calculated using Equation (26).

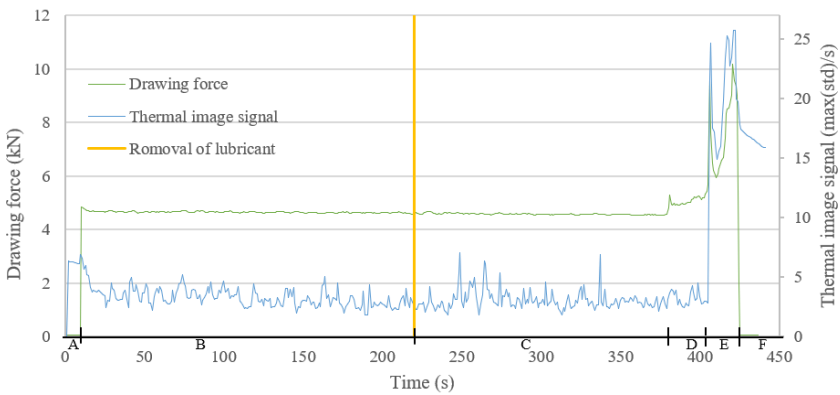

Figure 6.12. Drawing force and max standard deviation from thermal images for each second from the experiment. The experiment was divided into six regions, and they are discussed in the text. (Figure from Paper III)

The results could be divided into six regions. Region A is before the drawing process was started, the drawing force was 0 N and the signal

from the thermal camera was stable. The transition from region A to B indicates where the wire drawing process was started. In region B, the wire drawing process is functioning as intended, with functional lubrication, the coefficient of friction was calculated to 0.07 using Equation (16). The transition from region B to C is where the lubricant was removed. The behavior in region C does not display an increase in the drawing force signal, however, some clear spikes can be seen in the signal from the thermal imaging camera. At the transition from region C to D the lubrication in the process has partly failed, which is indicated in the drawing force signal. The transition from region D to E is where the degradation in lubrication performance is detected by the thermal image signal. The coefficient of friction went up to over 0.3 before the wire drawing process was stopped, transition E to F.

To evaluate the method for in-situ lubrication performance monitoring using wire temperature presented in chapter 5.2.2.1, the coefficient of friction was calculated and compared using the data from the experiment. Coefficient were calculated using Equation (16) (drawing force) and Equation (23) (wire temperature). To be able to use the data captured by means of thermal imaging, the emissivity of the wire needs to be known in order to get the actual temperature. For this reason, the emissivity of the wire surface was measured in the different regions, this was done by heating the wire and using a tactile temperature measurement equipment at the same time as the emissivity constant of the thermal imaging camera was iterated, until both measuring devices indicated the same temperature. In region B the emissivity of the wire surface was measured to 0.4 and in region E to 0.25. In region B the mean wire temperature is 103 °C and in region E the mean temperature is 156 °C. The coefficient of friction was calculated using both the drawing force and the adjusted with respect of emissivity wire temperatures, this is shown in *Figure 6.13*. The constant k in Equation (23) was set to 1 as no cooling of the drawing die was used during the experiment. As can be seen the two different ways to evaluate the performance of the lubrication seems to be in good agreement.

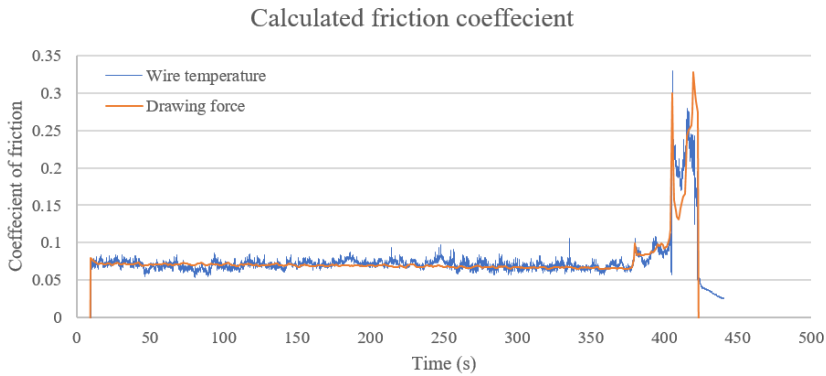

Figure 6.13. Friction coefficient calculated for the experiment. The coefficient has been calculated using the drawing force with Equation 16 and the wire temperaturewith Equation 23 respectively. (Figure from Paper III)

To couple the monitoring data with the characteristics of the produced wire, wire samples were collected from the different stages of the experiment and characterized by means of SEM. The wire surface from region B, C and E is shown in *Figure 6.14-6.16*. Surface analysis of the stainless-steel wire from region B and C revealed surface asperity flattening. Additionally, in region C a large scratch with width of approximately 500 µm was observed. In the scratched region, protrusions rising above the surface were observed, *Figure 6.15b*. Surface analysis of the wire from region E show a completely damaged surface and the protrusions were the main wear pattern seen in *Figure 6.16*.

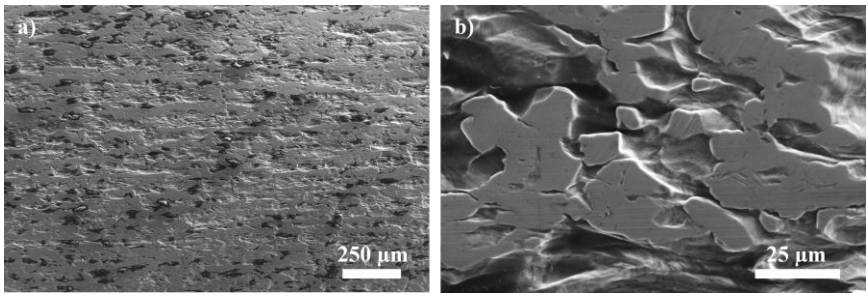

Figure 6.14. Surface of the stainless-steel wire in region B (functional lubrication) a) and magnification of the wire surface in region B displaying surface asperity flattening b). (Figure from Paper III)

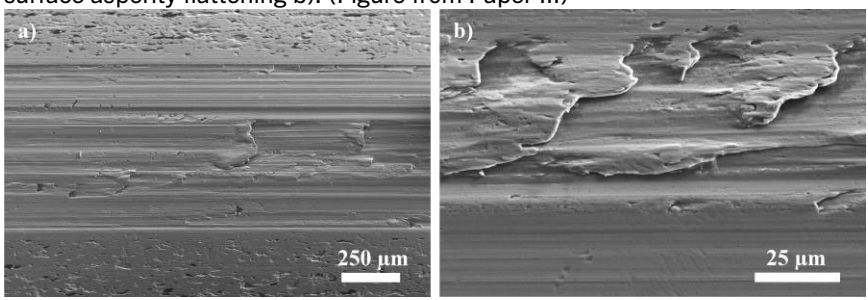

Figure 6.15. Wire surface from region C (no lubricant in die box). One scratch can be seen on the wire surface and the surface beside the scratch is like the surface in region B (Figure from Paper III)

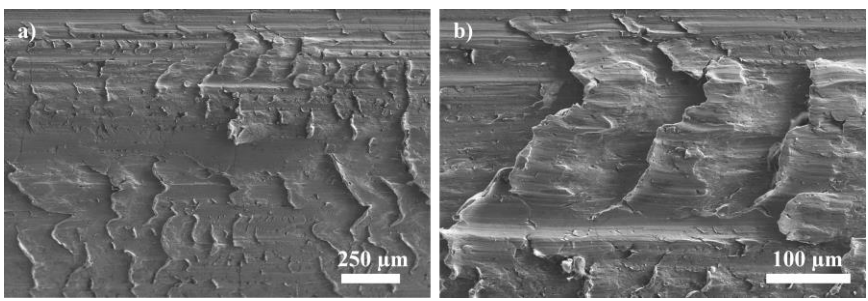

Figure 6.16. The typical surface of the wire in region E (unfunctional lubrication) illustrating the observed protrusions in SEM at magnifications of x70 a) and x1000 b) (Figure from Paper III)

Surface roughness measurements of the wire in region B, C and E were also carried out to correlate the monitoring signals with the produced wire surface characteristics. The measurements were made using a tactile surface roughness equipment. The result is presented in *Figure 6.17-6.18*. The mean roughness of the wire was $R_a = 1.09\ \mu m$ in region B, $R_a = 0.98\ \mu m$ in region C and $R_a = 6.13\ \mu m$ in region E. The scratch that was found in region C in the microscopy (*Figure 6.15*) is also detected in the surface roughness measurements (*Figure 6.18b*). The surface measurement in *Figure 6.18c* shows that the wire from region E is heavily damaged.

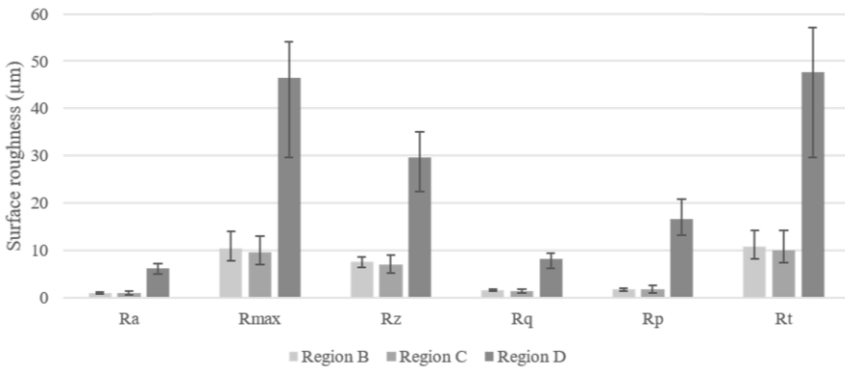

Figure 6.17. Surface roughness measurement values from the different regions of the experiment. (Figure from Paper III)

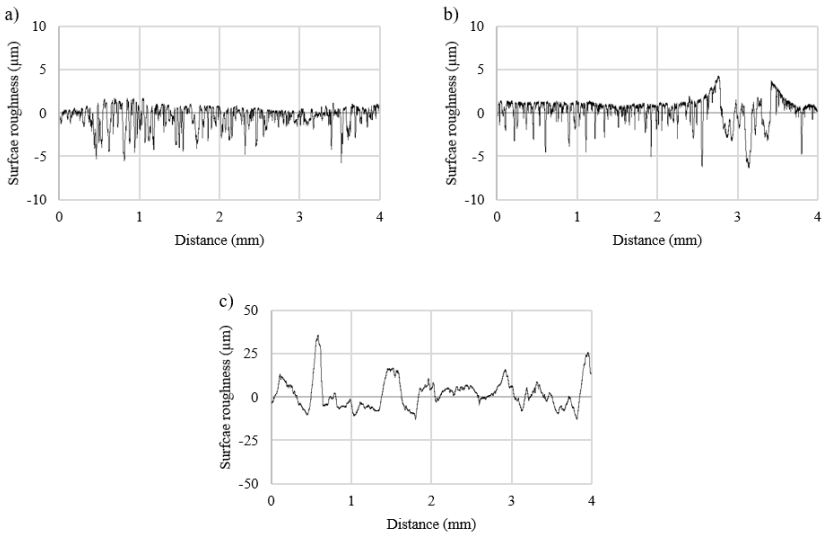

Figure 6.18. Example surface roughness measurements of the stainless-steel wire in a) region B (functional lubrication) b) region C (no lubricant in die box) and c) region E (unfunctional lubrication). The surfaces were measured along the curvature of the wire. (Figure from Paper III)

The two developed and evaluated process monitoring signals utilizing thermal measurements correlates very well with both the drawing force and the characteristics of the drawn wire.

6.4 Brightness measurements

To investigate the method presented in chapter 5.2.3, meaning that process issues can be captured with a camera in the same manner as the machine operators do today, the research study presented in Paper IV was conducted.

To test the hypotheses the wire brightness measurement sensor presented in chapter 5.2.3.1 was used. Experiments were carried out in the same manner as explained in chapter 6.3 and the data and resulting wire were analyzed and compared. Experiments were done using two different wire materials. In this chapter one of the experiments will be presented, the reader is referred to Paper IV for the second case. A stainless-steel (X10 CrNi 18-8 HS) wire was drawn. The experimental setup used to carry out the trials is shown in *Figure 6.19*.

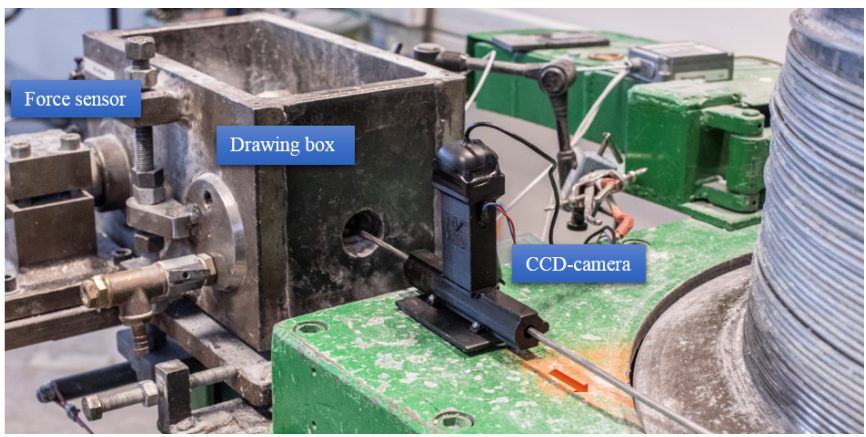

Figure 6.19. Experimental setup, brightness measuring equipment is placed after the wire exits the drawing die. (Figure from Paper IV)

The resulting monitoring signals from the experiment, the CCD-camera intensity calculated using Equation (27) and drawing force signal from the experiment are presented in *Figure 6.20*. Four regions could be observed in the monitoring data. Region A is before the drawing process was started, the drawing force was 0 N and the

intensity 150. The transition from region A to B indicated where the wire drawing process was started. In region B, the wire drawing process was functioning as intended, with lubrication, the coefficient of friction was calculated to 0.049. The transition from region B to C is where the lubrication was removed. The behavior of region C displays a constant increase of drawing force, and a constant decline in intensity. The friction coefficient increased up to 0.18 before the drawing was stopped. The two signals correlate very well and the transition from lubricated to non-lubricated process could clearly be detected in both signals. The transition from region C to D indicates where the wire drawing process was stopped.

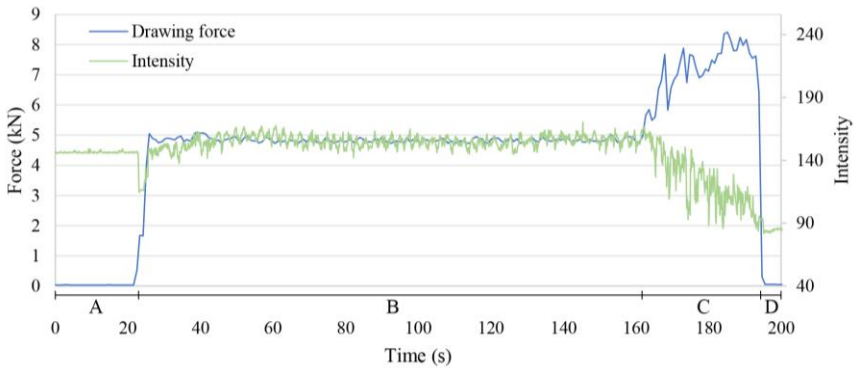

Figure 6.20. Drawing force and measured brightness (intensity). Four regions can be seen in the signals. (Figure from Paper IV)

To be able to correlate the measured process signals with the produced wire characteristics, wire samples were collected from region B (the lubricated region) and region C (non-functioning lubrication). These wire samples were analyzed and characterized by means of tactile surface roughness measurement and SEM. The wire surface from region B and C captured by SEM can be seen in *Figure 6.21*. The surface morphology of the wire in region B displays a smooth surface without signs of wear. In region C, however, there are severe signs of wear. Surface roughness profiles of the wire in region B and C can be seen in *Figure 6.22*. The roughness of the wire was $R_a = 1.09\ \mu m$ in the lubricated region and $R_a = 2.30\ \mu m$ in the unlubricated region.

This shows that the evaluated process monitoring method, brightness of the wire, correlates very well with both the drawing force signal as well with the characteristics of the produced wire.

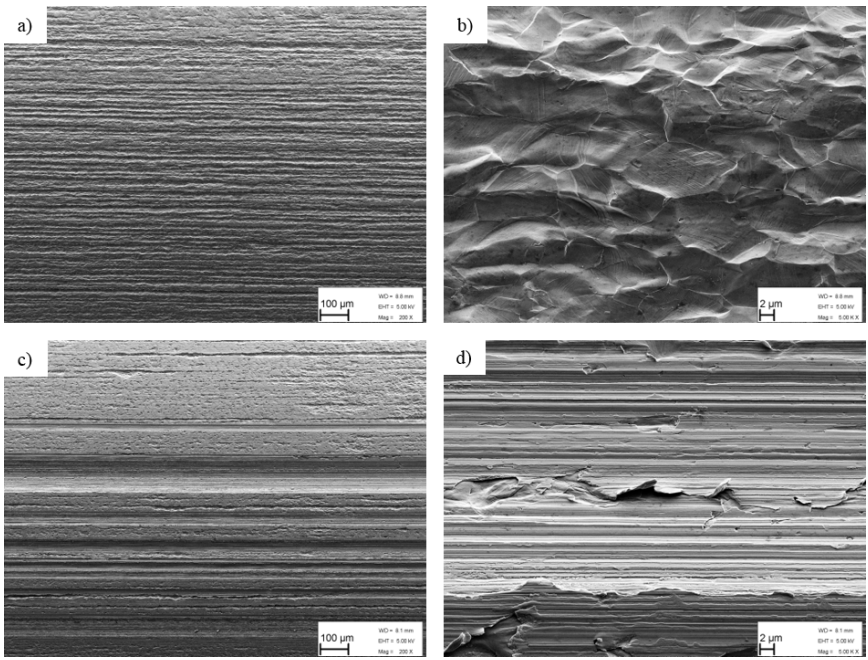

Figure 6.21. a) Surface of the wire in region B b) magnification of the wire surface in region B, free from signs of wear c) the surface of the wire in region C, displaying severe scarring d) magnification of the wire from region C, displaying a scratched surface (Figure from Paper IV)

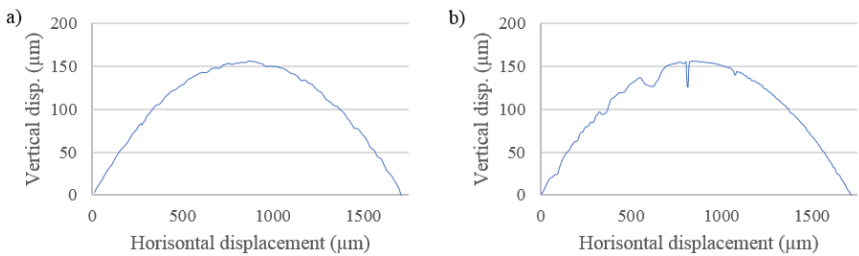

Figure 6.22. Surface profiles of the wire in a) region B and b) region C (Figure from Paper IV)

6.5 Multiple sensor approach - WiSE

In an effort to make research results available to the industry, researchers at Örebro University combined the monitoring methods presented in this thesis, and developed a monitoring system for the wire drawing process [76], [77]. The sensor utilizes the methods developed and evaluated within this thesis i.e. vibration measurement by means of accelerometer, wire brightness measurement using CCD-sensors and optical wire temperature measurements.

Some of the development stages are shown in *Figure 6.23*. The figure shows three prototype versions of the sensor installed in the wire drawing machine at Örebro University, as can be seen the physical footprint of the sensor has been gradually reduced to enable it to be used in most drawing machines.

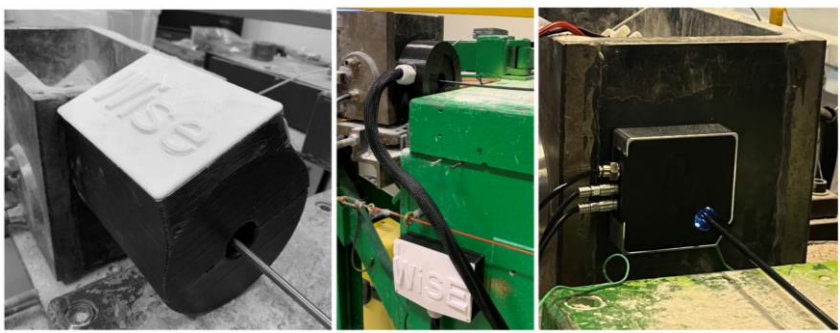

Figure 6.23. Three prototypes of WiSE process monitoring system for the wire drawing process.

The sensor was named Wire Surveillance Equipment, WiSE [78], and has been tested and evaluated in many scenarios, both in laboratory environments and in the industry. The sensor is installed at the exit side of the die box and the wire passes through the sensor. As the wire passes through, three cameras take images of the wire surface, which gives full image coverage of the surface. The sensor data is transferred by cable or Wi-Fi to a server where the data is analyzed and presented in a graphical user interface, shown in *Figure 6.24*. Each produced coil is automatically stored in a separate datafile for easy accessibility. To

ensure full trackability, the system can be equipped with a speed-sensor/signal, meaning that every meter of wire can be traced when looking for deviations in the monitoring signals. This also means that the system can be used as input for an Overall Equipment Efficiency (OEE) system.

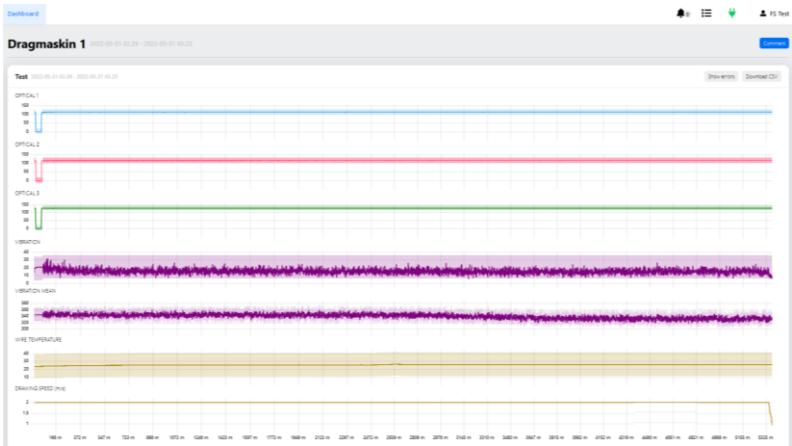

Figure 6.24. WiSE interface showing sensor data.

As suggested in Paper II-IV a threshold could be suitable to use to trigger an alarm/stop the machine, this is implemented in the WiSE-monitoring system. As seen in the results presented in paper III and IV the monitoring signal level can change significantly depending on the produced wire product. To solve this problem, the thresholds are set from a mean value which is calculated every time a new production run is started. The sensor utilizes the vibration measurement to get the information of when a production run is started and stopped to achieve fully functionality without the need for the machine operator to interact with the system. The “final” product is shown in *Figure 6.25* where it is installed in an industrial wire drawing machine in Japan.

Figure 6.25. WiSE-sensor in an industrial wire drawing machine.

Paper V was made to investigate what benefits that might exist by using multiple sensors for monitoring of the wire drawing process. The sensors used in the experiments were the WiSE sensor (vibration, brightness of the wire and wire temperature) and drawing force sensors, see *Figure 6.26*. Several different experiments were performed all using a carbon steel spring wire, the process conditions were changed during the experiments to mimic common problems of the wire drawing process, of which three are presented in this chapter.

Running out of lubricant

During this experiment the lubricant was left to run out naturally. This is a problem that can occur in industry when the operator is not able to keep a good level of lubricant in the drawing box or if other problems occur such as tunneling in the lubricant or blockage at the die entrance. The experiment was allowed to run until the drawing force reached elevated levels.

Issues from previous draws

This experiment mimics problems with previous draws in the process and was done to investigate if problems in draws prior to the draw being monitored can be detected. To simulate this the incoming wire

had an increased temperature for a period of time, creating problems with the performance of the lubricant in the investigated draw. This is a problem, which can occur for several different reasons: problems in the prior draw such as die damages, insufficient lubrication, die cooling not working and others. The problem can also occur when trying to increase the productivity, due to the increased drawing speed, the wire does not cool down enough on the capstan prior to the drawing die (as explained in *Figure 3.1*). This is a common industrial problem due to the demand of higher productivity. The increase in temperature of the ingoing wire was created by heating the wire using induction heating, this was done since there is only one draw in the laboratory setup used for the experiments. The temperature was increased to roughly 100°C and was constant throughout the heating period.

Long shallow cosmetic artificial defect

During this experiment the wire surface was subjected to grinding using a handheld angle grinder. This created a very shallow scratch, the scratch was not possible to feel by hand, neither before nor after the wire was drawn. This simulates a scratch created in a previous draw to the draw being monitored or in previous processes to the drawing process such as handling or heat treatment.

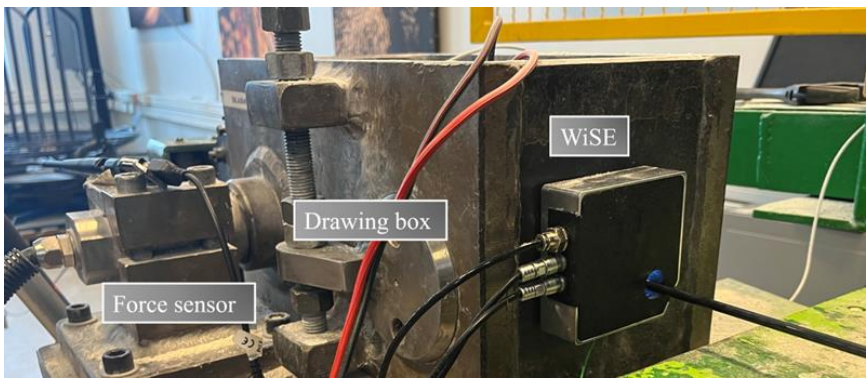

Figure 6.26. Experimental setup used in the trials. (Figure from Paper V)

6.5.1 Results

The experiments presented in section 6.5 were performed using the same type of lubricant, meaning that the coefficient of friction should be similar in all the performed experiments when there is a good lubrication situation. When comparing the drawing force from the experiments it was found that this was the case, the mean value from each of the experiments in the lubricated parts was 9100 ± 100 N. Using Equation (16) a corresponding coefficient of friction of 0.05 could be calculated, which is in the range 0.01-0.07 given in the literature as normal for a well lubricated dry drawing process [36], [51]. In some of the experiments the signal representing the wire temperature shows a slight increase throughout the experiment, this is probably because the wire drawing process had not yet reached steady state temperature when the experiment was performed.

Running out of lubricant

During the experiment a critical low level of lubricant was left to be present at the start of the experiment, and the process then ran until the force level reached elevated levels. The result from the experiment is shown in *Figure 6.27*, displaying vibration, wire temperature, optical signal and drawing force. The vibration, wire temperature and drawing force signals show a similar behavior. All signals indicates that there are some changes in the process from around 225 seconds. This is likely due to the change in lubrication performance due to the lack of lubricant. The coefficient of friction increases from 0.05 up to 0.16 at the end of the experiment. The optical signal, representing the brightness of the wire, shows that this signal detects the coming issue before the other signals. This is probably because the brightness of the wire changes (due to the lack of lubricant) before the loss of lubricant affects the friction of the system. This means that the brightness of the wire could be used to prevent the process of getting to a poorly lubricated state, since it gives an indication before the drawing force increases. In this experiment, the process was stopped before any damage occurred in the tool or on the drawn wire, there was also no indication that could be detected by the machine operator that there would be any problem in the process.

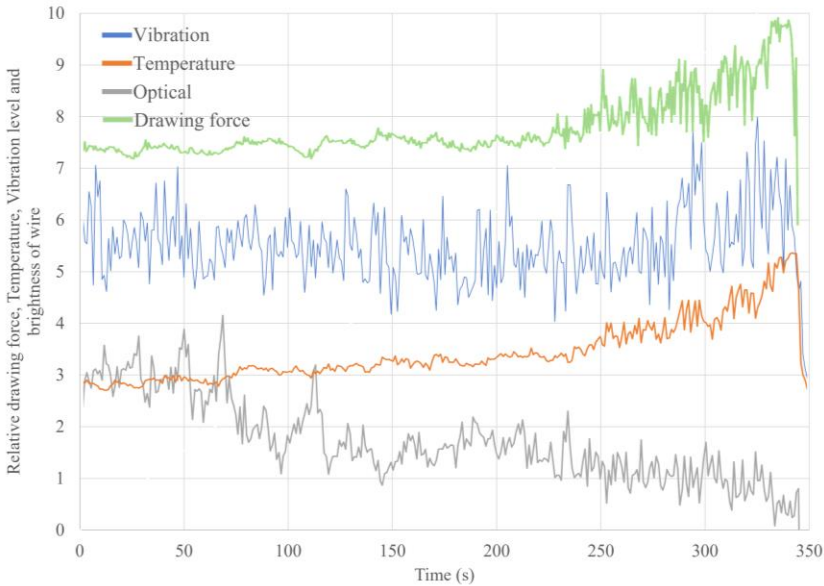

Figure 6.27. Results from the experiment where the lubricant was let to run out. The figure shows the four measured signals, Vibration, Wire temperature, wire brightness (Optical) and drawing force. (Figure from Paper V)

Issues from previous draws

Figure 6.28 presents the results from the experiment simulating a problem in a previous draw, leading to increased ingoing wire temperature.

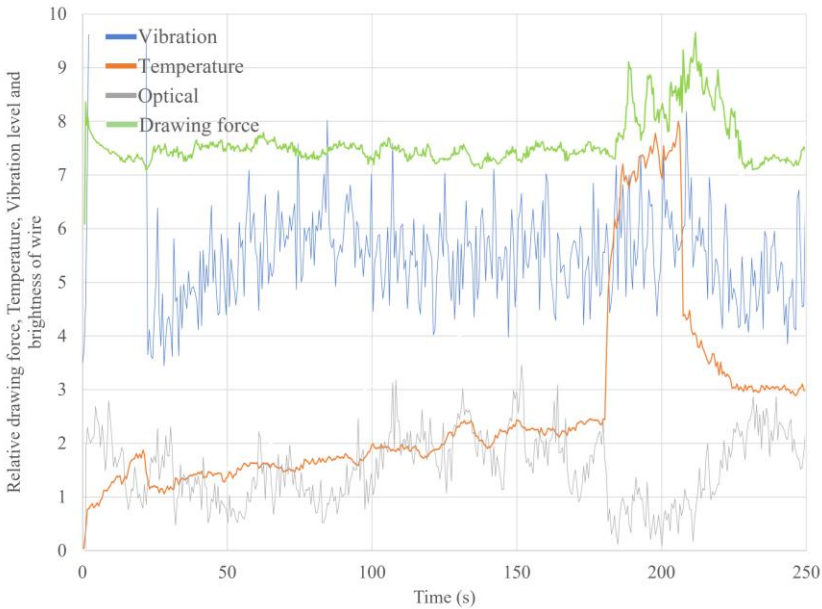

Figure 6.28. Results from the experiment simulating problem in a previous draw to the one being monitored. The figure shows the four measured signals, Vibration, Wire temperature, wire brightness (Optical) and drawing force. (Figure from Paper V)

As shown in the figure, the wire section with increased temperature reaches the process after around 180 seconds, the problem is restored, and the wire is restored to normal conditions at around 210 seconds. The temperature of the ingoing wire was increased to roughly 100°C during that time. The increase in temperature seems to have led to some problems with the lubrication, as shown by the increase in drawing force indicating an increase in the coefficient of friction, the coefficient increases to 0.12. The problem occurring in the process could also be detected by analyzing the optical signal as well as by the drawn wire temperature signal. When the temperature decreases the process is going back to a normal state. There is a delay from when the ingoing wire temperature goes down until the temperature of the drawn wire is back to normal, this is due to the cooling of the drawing die, it takes some time for it to return to normal temperature. No damage could be detected on either the tool or the

wire, and the operator could not detect any problem with the performance of the drawing process.

The result show that it would be possible to detect a problem in a draw previous to the monitored draw.

Long shallow cosmetic artificial defect

Figure 6.29 shows the resulting scratch after passing through the drawing die, the scratch is very shallow and cannot be felt by hand.

Figure 6.29. Shallow artificial scratch after being reduced in the drawing die.

The resulting monitoring data from the experiment is presented in *Figure 6.30.*

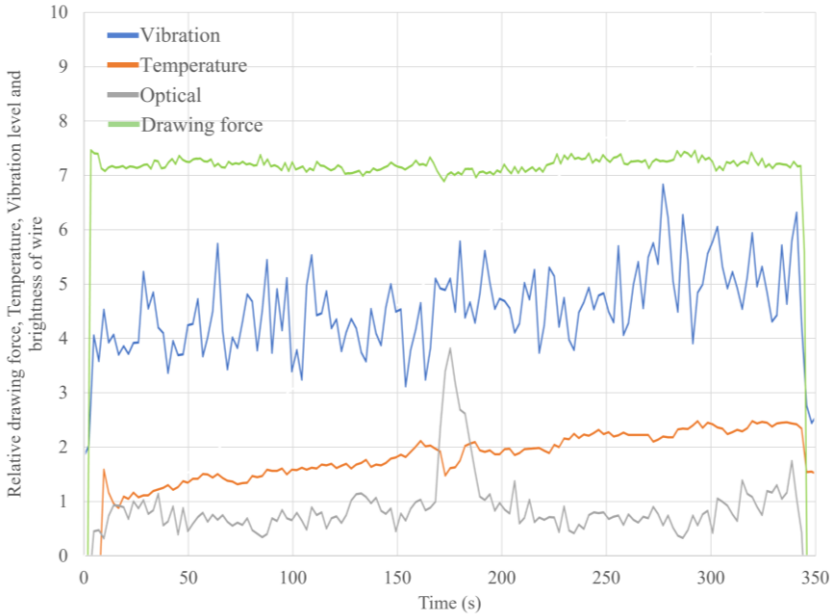

Figure 6.30. Results from the experiment where an artificial cosmetic scratch investigated. The figure shows the four measured signals, Vibration, Wire temperature, wire brightness (Optical) and drawing force.

The scratch passes through the drawing die after around 160 seconds, which clearly shows on the optical signal, a small indication can also be seen on the temperature signal. The difference in temperature is probably not due to an actual change in wire temperature, since the scratch is very shallow but due to the change in emissivity, the scratch is much brighter than the undamaged wire surface, which can be seen from the increase in the optical signal. As the wire surface becomes brighter the measured temperature value gets lower.

Running the drawing process without cooling until problems can be detected by machine operator

The earlier experiments showed that the monitoring sensors could detect performance problems occurring in the drawing process without it being noticeable for the machine operator. No defects

could be detected on the wire or the drawing die after the performed experiments where the lubrication performance was degraded. This experiment was performed to see how serious the performance changes must be to be able to be detected by the machine operator. The process was run without cooling and the temperature of the ingoing wire was increased during the experiment. The experiment was stopped when the operator noticed problems in the process, the result from the experiment is presented in *Figure 6.31.*

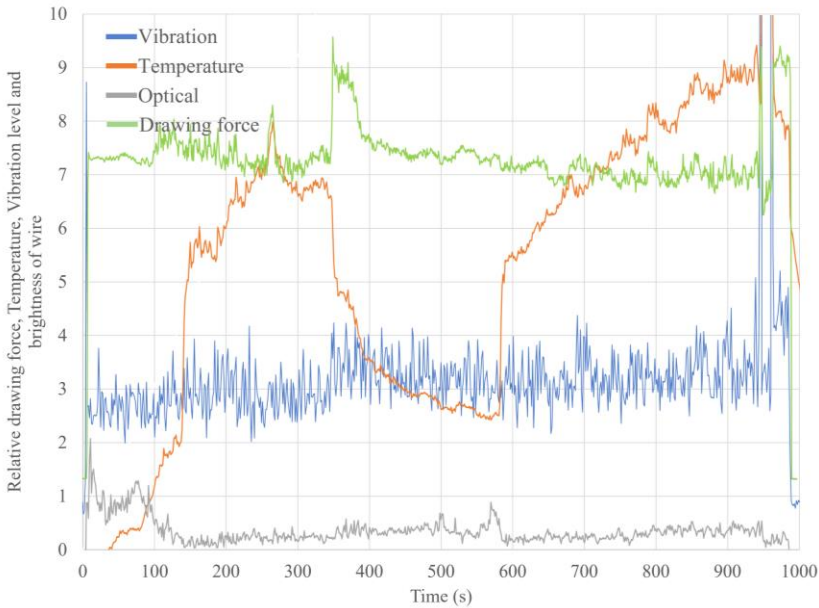

Figure 6.31. Results from the experiments where the process was let to run without cooling until the operator would detect that there is a problem in the process. The figure shows the four measured signals, Vibration, Wire temperature, wire brightness (Optical) and drawing force.

At the beginning of the experiment the process was left to run in a normal state, after 150 seconds the ingoing wire temperature was increased to 100 °C. This increase in temperature results in a less favorable lubrication situation, which is indicated by all the used sensors. After 200 seconds the cooling of the drawing die is removed which also leads to an increased temperature of the drawn wire. After

approximately 100 additional seconds, the lubrication performance degrades further for a short period of time which is indicated by the wire temperature and the drawing force measurements. At 400 seconds the ingoing wire temperature is decreased to room temperature, this somehow leads to even an even worse lubrication performance for a while, which is indicated by the drawing force signal. At 600 seconds the lubrication seems to start to stabilize due to the decrease in tool temperature, at this point the ingoing wire temperature is increased from room temperature up to 100 °C again, which is indicated by the increase in wire temperature. After around 950 seconds the temperature in the tool has increased to levels which causes the lubrication to completely malfunction, which is indicated by all the monitoring signals. The coefficient of friction is at this point 0.16 and the process is allowed to continue. The vibration level and wire temperature are not ideally displayed in Figure 39, but the level is more than 200 times higher for the vibration signal compared to the mean value from the rest of the experiment and the temperature signal is roughly twice as high as displayed. At this point, the problems in the process could be detected by the machine operator due to a strange noise from the drawing die and the process was stopped. When optical inspecting the wire after the experiment, the wire surface seems to be brighter, but it is difficult to tell when studying the wire with the human eye.

From the results of the experiment, it is clear that the monitoring signals can detect process performance problems long before they become a real issue. The monitoring sensors were able to detect problems in the process around 900 seconds before the operator could notice anything unusual with the process, meaning that if process monitoring is utilized in the industrial process, problems could be detected and corrected a long time before they actually start to cause real problems.

7 Conclusions

This chapter provides concluding remarks on the results from this thesis and answers to the questions presented in chapter 1.2.

7.1 General conclusions and future work

It was found that process monitoring can be a helpful tool to increase the sustainability and productivity in the wire drawing industry. By the use of monitoring sensors, it is possible to detect process problems before damage is manifest on the tools and the wire, meaning that material can be saved from being scrapped. Also, information from the sensors can be used to optimize the production processes, as limits for the used tooling and lubrication can be found.

All investigated monitoring methods had close correlation to the drawing force which has been previously demonstrated to give indications of the status of the wire drawing process. Also, it was shown that surface damage due to poor lubrication could be correlated to deviations in the monitoring data.

As shown in paper V, using multiple sensors might have an advantage because the error misclassification should be less of a problem, since the different monitoring methods react in a similar way to the evaluated performance issues.

A way that might increase the knowledge of what is happening in the drawing process using data from the sensors evaluated in this thesis would be by the use of machine learning. It might be possible to develop a model of how the different monitoring signals react to different type of process problems, meaning that a specific type of problem could be detected. It would also be very interesting to study if it is possible to develop a model that could control and optimize the drawing process using the monitoring data as input.

7.2 Answers to specific industrial and research questions

To remind the reader of the questions stated in chapter 1.2 the industrial and research questions are listed below with formulated answers.

Is it possible to detect problems in the wire drawing process by using process monitoring that can be implemented in an existing industrial wire drawing machine??
As shown in chapter 6 (Paper II-V) it is possible to detect problems in a wire drawing process by using the methods developed within this thesis. All methods have been developed considering that they should be easily implemented in existing equipment. The sensor system presented in chapter 6.5 which builds upon the developed methods is a step towards industrial implementation of process monitoring in the wire drawing process.

Can problems be detected before they become an issue?
The results from the performed studies show that there is high potential to detect performance problems before they become an issue causing damages to the wire and tools. This of course depends on the drawing process and how sensitive the wire material is to galling.

Can the efficiency of the process be estimated using sensors?
It was shown that a performance index, the coefficient of friction, can be calculated which represents the lubrication performance. A method to calculate this performance indicator using the wire temperature was proven to be viable (Equation (23)).

Are there measurable process parameters in the wire drawing process that reflect the properties of the produced wire??
All the evaluated process monitoring methods were found to reflect the characteristics of the produced wire at a comprehensible level, which means that the monitoring signals can indicate whether there is damage or not.

Can process signals be linked to material characteristics?
The studied process monitoring signals can indicate at a superficial level what is happening on the wire surface. However, to be able to identify what type of specific defect is on the surface of a certain type of wire in a certain process, the specific process must be investigated.

8 Acknowledgements

My journey towards the end of my doctoral studies has been very long, and many people to whom I owe my gratitude have been involved along the way. First of all, I would like to thank Professor Magnus Jarl who encouraged me to stay in academia after graduation. I would also like to thank Professor Lars Pejryd, whose positive and encouraging attitude made me return to academia. A special thanks also goes to Professor Rachel Pettersson for her outstanding support, without her this doctoral thesis would not have been possible.

I am also grateful to my main supervisor Christer Korin for his support and nice conversations. Acknowledgement also goes to Anton Jansson for being a co-supervisor, partner-in-crime and a funny guy, and to my co-supervisor/traveling buddy Patrik Karlsson; getting to work with you guys has been very rewarding.

I am also very thankful to have had the opportunity to work in wire drawing research projects for more than 12 years together with Peter Gillström, whose support never fails. Thanks also go to all of the co-authors of the research studies and my colleagues at the university, especially Per.

My appreciation also goes to the wire drawing companies that have participated in the research work associated with this thesis; ESAB, Fagersta Stainless, Hjulsbro Steel, Hörle Wire, Kanthal, Suzuki Garphyttan and Zapp Precision Metals. It has been a great joy working together, doing research in a real environment. I am also grateful to the organizations whose financial support made the research behind this doctoral thesis possible, Vinnova, The Knowledge Foundation (KK-Stiftelsen), Jernkontoret and Hugo Carlsson's Foundation.

And last but not least, I want to thank my partner Liza and our lovely kids for putting up with me, especially during the last year of my doctoral studies.

9 References

[1] *Gamla testamentet*. 2000.

[2] J. Webster and R. T. Watson, "Analyzing the Past to Prepare for the Future: Writing a Literature Review.," *MIS Q.*, vol. 26, no. 2, pp. xiii–xxiii, 2002.

[3] D. Tranfield, D. Denyer, and P. Smart, "Towards a Methodology for Developing Evidence-Informed Management Knowledge by Means of Systematic Review," *Br. J. Manag.*, vol. 14, no. 3, pp. 207–222, 2003.

[4] C. F. Durach, A. Wieland, and J. A. D. Machuca, "Antecedents and dimensions of supply chain robustness: A systematic literature review," *Int. J. Phys. Distrib. Logist. Manag.*, vol. 45, pp. 118–137, 2015.

[5] N. M. Agnew and S. W. Pyke, *The Science Game: An Introduction to Research in the Social Sciences 7th edition*. Oxford: Oxford University Press, 2007.

[6] K. Säfsten and M. Gustavsson, *Forskningsmetodik : för ingenjörer och andra problemlösare*, Upplaga 1. Lund: Studentlitteratur, 2019.

[7] LabVIEW, "2013 version 13.0.1." National Instruments, 2014.

[8] L. E. Persson, "A short history of wire drawing," *Wire Ind.*, vol. 72, no. 859, pp. 387–390, 2005.

[9] M. Nilsson and M. Olsson, "On the possibility to replace cemented carbide with CVD and PVD coated steel in wire drawing dies--A tribological investigation," in *Wear of Materials, Las Vegas, 19-23 april, 2009*, 2009.

[10] M. Nilsson and M. Olsson, "Tribological testing of some potential PVD and CVD coatings for steel wire drawing dies," *Wear*, vol. 273, no. 1, pp. 55–59, 2011.

[11] K. B. Surreddi and M. Olsson, "Wear of cemented carbide nibs in steel wire drawing," in *The 18th Nordic Symposium on Tribology--NORDTRIB 2018, 18-21 June 2018, Uppsala University, Uppsala, Sweden*, 2018.

[12] M. Olsson and K. B. Surreddi, “Scratch testing of cemented carbides-Influence of Co binder phase and WC grain size on surface deformation and degradation mechanisms,” in *18th Nordic Symposium on Tribology-Nordtrib 2018*, 2018.

[13] K. B. Surreddi, J. Larsson, and M. Olsson, “Investigating the surface degradation and wear mechanisms of uncoated and PVD-coated cemented carbide dies in steel wire drawing,” in *Tooling2022*, 2022, pp. 523–530.

[14] “Nano-Die.” [Online]. Available: https://www.nano-die.com.au/.

[15] “Esteves.” [Online]. Available: https://www.estevesgroup.com/.

[16] “Ballofet.” [Online]. Available: https://balloffetdie.com.

[17] “Fort Wayne Wire Die.” [Online]. Available: https://www.fwwd.com/.

[18] “Vassena.” [Online]. Available: https://www.vassena.it/.

[19] L. Pejryd and J. Larsson, “Additively manufactured tool holder for wire drawing processes,” in *EURO PM2018 Congress Proceedings :*, 2018.

[20] J. Larsson, P. Karlsson, J. Ekengren, and L. Pejryd, “Enhanced Cooling Design in Wire Drawing Tooling Using Additive Manufacturing,” in *Industrializing Additive Manufacturing Proceedings of AMPA2020*, 2020, pp. 426–436.

[21] J. Larsson, B. Chetroiu, and E. Enghag, “Additively manufactured conformal cooling tool holder for wire drawing uti- lizing triply periodic minimal surfaces,” in *Tooling2022*, 2022, pp. 22–29.

[22] J. Larsson, S. Garmendia Alustiza, N. Otegi, and P. Karlsson, “Enhanced cooling by conformal cooling of additively manufactured wire drawing tools made of cemented carbide,” in *MAMC2022*, 2022, pp. 225–235.

[23] J. Larsson and M. Jarl, “Högre draghastigheter / Temperaturens inverkan,” *NTTF*, pp. 51–58, 2011.

[24] G. Vega, A. Haddi, and A. Imad, “Investigation of process parameters effect on the copper-wire drawing,” *Mater. Des.*,

vol. 30, no. 8, pp. 3308–3312, 2009.

[25] I. M. Sas-Boca, M. Tintelecan, M. Pop, D. A. Iluțiu-Varvara, and A. M. Mihu, "The Wire Drawing Process Simulation and the Optimization of Geometry Dies," *Procedia Eng.*, vol. 181, pp. 187–192, 2017.

[26] T. Massé, L. Fourment, P. Montmitonnet, C. Bobadilla, and S. Foissey, "The optimal die semi-angle concept in wire drawing, examined using automatic optimization techniques," *Int. J. Mater. Form.*, vol. 6, no. 3, pp. 377–389, 2013.

[27] M. Tintelecan, I. M. Sas-Boca, and D. A. Iluțiu-Varvara, "The influence of the dies geometry on the drawing force for steel wires," *Procedia Eng.*, vol. 181, pp. 193–199, 2017.

[28] J. Toribio, M. Lorenzo, and D. Vergara, "On the use of varying die angle for improving the resistance to hydrogen embrittlement of cold drawn prestressing steel wires," *Eng. Fail. Anal.*, vol. 47, no. PB, pp. 273–282, 2015.

[29] J. Toribio, M. Lorenzo, D. Vergara, and V. Kharin, "Influence of the die geometry on the hydrogen embrittlement susceptibility of cold drawn wires," *Eng. Fail. Anal.*, vol. 36, pp. 215–225, 2014.

[30] H. Överstam, "The influence of bearing geometry on the residual stress state in cold drawn wire, analysed by the FEM," *J. Mater. Process. Technol.*, vol. 171, no. 3, pp. 446–450, 2006.

[31] L. K. Kabayama *et al.*, "The Influence of Die Geometry on Stress Distribution by Experimental and FEM Simulation on Electrolytic Copper Wiredrawing," *Mater. Res.*, vol. 12, no. 3, pp. 281–285, 2009.

[32] A. R. Bandar, R. B. Gifford, W. Z. Misiolek, and J. P. Coulter, "Impact of die geometry on microhardness and grain size of cold-drawn steel wire," *Mater. Manuf. Process.*, vol. 19, no. 3, pp. 507–521, 2004.

[33] J. Adamczyk, M. Suliga, J. W. Pilarczyk, and M. Burdek, "The influence of die approach and bearing part of die on mechanical-technological properties of high carbon steel wires," *Arch. Metall. Mater.*, vol. 57, no. 4, pp. 1105–1110, 2012.

[34] M. Suliga, M. Jabłońska, and M. Hawryluk, “The effect of the length of the drawing die sizing portion on the energy and force parameters of the medium-carbon steel wire drawing process,” *Arch. Metall. Mater.*, vol. 64, no. 4, pp. 1353–1359, 2019.

[35] Paramount, “www.paradie.com.” .

[36] P. Enghag, *Steel Wire Technology*. Örebro: Materialteknik HB, 2009.

[37] J. Larsson, P. Karlsson, and L. Pejryd, “The effect of bearing length on the surface quality of drawn wires,” *Wire J. Int.*, vol. 53, no. February, pp. 50–55, 2020.

[38] K. El-Amine and L. Pejryd, “Study and optimization of changeover procedures in wire drawing,” in *7th Swedish Production Symposium (SPS 16)* :, 2016.

[39] J. . Archard, “Contact and Rubbing of Flat Surfaces,” *J. Appl. Phys.*, vol. 24, pp. 981–988, 1953.

[40] J. . Wistreich, “The fundamentals of wire drawing,” *Metall. Rev.*, vol. 3, no. 10, pp. 97–142, 1958.

[41] T. H. Kim, B. M. Kim, and J. C. Choi, “Prediction of die wear in the wire-drawing process,” *J. Mater. Process. Technol.*, vol. 65, no. 1–3, pp. 11–17, 1997.

[42] E. Siebel and R. Kobitzsch, “Die Erwärmung des Ziehgutes biem Drahtzienhen,” *Stahl und Eisen*, vol. 63, no. 6, pp. 110–114, 1942.

[43] O. . Sachs and G. Hoffman, *Introduction to the Theory of Plasticity for Engineers*. New York: McGraw-Hill BookCompany, 1953.

[44] R. N. Wright, *Wire Technology*. Elsevier Ltd, 2009.

[45] B. O. Haglund and P. Enghag, “Characterization of lubricants used in the metalworking industry by thermoanalytical methods,” *Thermochim. Acta*, vol. 282–283, no. SPEC. ISS., pp. 493–499, 1996.

[46] T. Morge, T. Srl, E. G. Garoli, and K. Srl, “SUSTAINABLE ADDITIVES TO INCREASE THERMAL STABILITY OF DRY

LUBRICANTS AND BEST PRACTISE OF USE," in *Wire & Cable Milan*, 2023, pp. 5–16.

[47] B. Avitzur, "Analysis of Wire Drawing and Extrusion Through Conical Dies of Large Cone Angle," *J. Eng. Ind.*, vol. 86, no. 4, pp. 305–314, 1964.

[48] B. Avitzur, *Metal forming: the application of limit analysis*. Dekker, 1980.

[49] B. Avitzur, *Handbook of metal-forming processes*. Wiley, 1983.

[50] L. Persson and P. Enghag, "Basic principles of wire drawing," *Wire Ind.*, no. October, pp. 727–733, 1996.

[51] R. Shemenski, *Ferrous wire handbook*. Guildford, Conn.: Wire Association International, 2008.

[52] M. Jarl and H. Överstam, "Simulation of temperatures in the wiredrawing process.," *Wire J. Int.*, no. February, pp. 150–155, 2008.

[53] J. Larsson, A. Jansson, and P. Karlsson, "Monitoring and evaluation of the wire drawing process using thermal imaging," *Int. J. Adv. Manuf. Technol.*, vol. 101, no. 5, pp. 2121–2134, 2019.

[54] R. N. Wright, "Physical conditions in the lubricant layer," *Wire J. Int.*, no. August, pp. 88–92, 1997.

[55] J. Larsson and M. Jarl, "Högre draghastighet," *NTTF Årsb.*, pp. 63–70, 2012.

[56] Sandvik, "Understanding Cemented Carbide The material with staying power." p. 20, 2011.

[57] "ASTM G40 Standard Teminology Relating to Wear and Erosion." 1999.

[58] P. Karlsson, P. Krakhmalev, A. Gåård, and J. Bergström, "Influence of work material proof stress and tool steel microstructure on galling initiation and critical contact pressure," *Tribol. Int.*, vol. 60, pp. 104–110, 2013.

[59] B. Nilsson and B. Stenlund, "Detection of lubrication failures in wire drawing," *Wire Ind.*, vol. 51, no. 611, pp. 855–858,

1984.

[60] T. Holm, K. E. Karlstrom, A. Philipson, and B. Nilsson, “Lubrication failures in wire drawing,” *Wire Ind.*, vol. 52, no. 616, pp. 242–245, 1985.

[61] B. Nilsson, “Die wear monitoring and control of drawing,” *Wire Ind.*, no. January, pp. 40–43, 1991.

[62] B. Nilsson, “In-process die wear diagnosis by contact resistance measurement,” *Wire J. Int.*, vol. 27, no. 6, pp. 76–80, 1994.

[63] B. Nilsson, “Diagnosing wire drawing processes by indirect measurements,” *WIRE*, vol. 2, no. April, pp. 70–73, 2001.

[64] B. Nilsson, “MODEL 83 TEARING DETECTOR SYSTEM.” pp. 1–12, 1984.

[65] N. C. Pease, “Flaw protection in wire drawing,” Patent number GB2137344A, UK., 1984.

[66] T. Sato, K. Yoshikawa, H. Okitsu, I. Morita, and M. Saga, “Assessment of Frictional Conditions by Acoustic-Emission Technique in Metal Formin,” *J. Jpn. Soc. Techn. Plast.*, vol. 21, no. 234, pp. 608–613, 1980.

[67] S. Masaki, T. Tabata, and K. Konishi, “Evaluation of Lubrication in Wire Drawing Using Acoustic Emission Method,” *J. Jpn. Soc. Techn. Plast.*, vol. 26, no. 295, pp. 835–841, 1985.

[68] S. Masaki, T. Tabata, B.-Q. Zuh, and H. Hayasashi, “A Method for Evaluating Lubricntion in Wire Drawing by Acoustic Emission Technique,” *J. Jpn. Soc. Techn. Plast.*, vol. 29, no. 334, pp. 1166–1171, 1988.

[69] U. Seuthe, “US 8,720,272 B2,” 2014.

[70] E. Caso, A. Diez-Ibarbia, P. Garcia, J. Sanchez-Espiga, and A. Fernandez-del-Rincon, “Evaluation of acoustic emission for monitoring wire drawing process,” *Mech. Syst. Signal Process.*, vol. 200, no. May, 2023.

[71] E. Caso, P. García-Fernández, A. Fernández-del-Rincón, A. De-Juan-De-Luna, A. Díez-Ibarbia, and J. Sánchez-Espiga, “Acoustic Emission Monitoring for Wire Drawing Process,” in

Advances in Technical Diagnostics II, 2023, pp. 52–62.

[72] J. Larsson, H. Johansson-Cider, and M. Jarl, "Monitoring of the wiredrawing process," in *Annual Convention of the Wire Association International Monitoring*, 2013, no. 83.

[73] Ansys, "2022 version R3." .

[74] FLIR Systems INC, "Flir a315 / a615," 2014.

[75] ResearchIR, "Version 3.4.13235." FLIR Systems Inc., 2011.

[76] J. Larsson, "Digitalisering i tråddragningsindustrin," in :, 2019, pp. 66–72.

[77] J. Larsson, A. Jansson, and L. Pejryd, "Wire 4.0," in :, 2019, pp. 185–198.

[78] A. Wire Innovations Sweden, "WiSE." [Online]. Available: https://wirein.se/.

Publications *in the series*
Örebro Studies in Technology

1. Bergsten, Pontus (2001) *Observers and Controllers for Takagi – Sugeno Fuzzy Systems*. Doctoral Dissertation.
2. Iliev, Boyko (2002) *Minimum-time Sliding Mode Control of Robot Manipulators*. Licentiate Thesis.
3. Spännar, Jan (2002) *Grey box modelling for temperature estimation*. Licentiate Thesis.
4. Persson, Martin (2002) *A simulation environment for visual servoing*. Licentiate Thesis.
5. Boustedt, Katarina (2002) *Flip Chip for High Volume and Low Cost – Materials and Production Technology*. Licentiate Thesis.
6. Biel, Lena (2002) *Modeling of Perceptual Systems – A Sensor Fusion Model with Active Perception*. Licentiate Thesis.
7. Otterskog, Magnus (2002) *Produktionstest av mobiltelefonantenner i mod-växlande kammare*. Licentiate Thesis.
8. Tolt, Gustav (2003) *Fuzzy-Similarity-Based Low-level Image Processing*. Licentiate Thesis.
9. Loutfi, Amy (2003) *Communicating Perceptions: Grounding Symbols to Artificial Olfactory Signals*. Licentiate Thesis.
10. Iliev, Boyko (2004) *Minimum-time Sliding Mode Control of Robot Manipulators*. Doctoral Dissertation.
11. Pettersson, Ola (2004) *Model-Free Execution Monitoring in Behavior-Based Mobile Robotics*. Doctoral Dissertation.
12. Överstam, Henrik (2004) *The Interdependence of Plastic Behaviour and Final Properties of Steel Wire, Analysed by the Finite Element Metod*. Doctoral Dissertation.
13. Jennergren, Lars (2004) *Flexible Assembly of Ready-to-eat Meals*. Licentiate Thesis.
14. Jun, Li (2004) *Towards Online Learning of Reactive Behaviors in Mobile Robotics*. Licentiate Thesis.
15. Lindquist, Malin (2004) *Electronic Tongue for Water Quality Assessment*. Licentiate Thesis.
16. Wasik, Zbigniew (2005) *A Behavior-Based Control System for Mobile Manipulation*. Doctoral Dissertation.

17. Berntsson, Tomas (2005) *Replacement of Lead Baths with Environment Friendly Alternative Heat Treatment Processes in Steel Wire Production*. Licentiate Thesis.

18. Tolt, Gustav (2005) *Fuzzy Similarity-based Image Processing*. Doctoral Dissertation.

19. Munkevik, Per (2005) *"Artificial sensory evaluation – appearance-based analysis of ready meals"*. Licentiate Thesis.

20. Buschka, Pär (2005) *An Investigation of Hybrid Maps for Mobile Robots*. Doctoral Dissertation.

21. Loutfi, Amy (2006) *Odour Recognition using Electronic Noses in Robotic and Intelligent Systems*. Doctoral Dissertation.

22. Gillström, Peter (2006) *Alternatives to Pickling; Preparation of Carbon and Low Alloyed Steel Wire Rod*. Doctoral Dissertation.

23. Li, Jun (2006) *Learning Reactive Behaviors with Constructive Neural Networks in Mobile Robotics*. Doctoral Dissertation.

24. Otterskog, Magnus (2006) *Propagation Environment Modeling Using Scattered Field Chamber.* Doctoral Dissertation.

25. Lindquist, Malin (2007) *Electronic Tongue for Water Quality Assessment*. Doctoral Dissertation.

26. Cielniak, Grzegorz (2007) *People Tracking by Mobile Robots using Thermal and Colour Vision*. Doctoral Dissertation.

27. Boustedt, Katarina (2007) *Flip Chip for High Frequency Applications – Materials Aspects*. Doctoral Dissertation.

28. Soron, Mikael (2007) *Robot System for Flexible 3D Friction Stir Welding*. Doctoral Dissertation.

29. Larsson, Sören (2008) *An industrial robot as carrier of a laser profile scanner: Motion control, data capturing and path planning*. Doctoral Dissertation.

30. Persson, Martin (2008) *Semantic Mapping Using Virtual Sensors and Fusion of Aerial Images with Sensor Data from a Ground Vehicle*. Doctoral Dissertation.

31. Andreasson, Henrik (2008) *Local Visual Feature based Localisation and Mapping by Mobile Robots*. Doctoral Dissertation.

32. Bouguerra, Abdelbaki (2008) *Robust Execution of Robot Task-Plans: A Knowledge-based Approach*. Doctoral Dissertation.

33. Lundh, Robert (2009) *Robots that Help Each Other: Self-Configuration of Distributed Robot Systems*. Doctoral Dissertation.

34. Skoglund, Alexander (2009) *Programming by Demonstration of Robot Manipulators*. Doctoral Dissertation.

35. Ranjbar, Parivash (2009) *Sensing the Environment: Development of Monitoring Aids for Persons with Profound Deafness or Deafblindness*. Doctoral Dissertation.

36. Magnusson, Martin (2009) *The Three-Dimensional Normal-Distributions Transform – an Efficient Representation for Registration, Surface Analysis, and Loop Detection*. Doctoral Dissertation.

37. Rahayem, Mohamed (2010) *Segmentation and fitting for Geometric Reverse Engineering. Processing data captured by a laser profile scanner mounted on an industrial robot*. Doctoral Dissertation.

38. Karlsson, Alexander (2010) *Evaluating Credal Set Theory as a Belief Framework in High-Level Information Fusion for Automated Decision-Making*. Doctoral Dissertation.

39. LeBlanc, Kevin (2010) *Cooperative Anchoring – Sharing Information About Objects in Multi-Robot Systems*. Doctoral Dissertation.

40. Johansson, Fredrik (2010) *Evaluating the Performance of TEWA Systems*. Doctoral Dissertation.

41. Trincavelli, Marco (2010) *Gas Discrimination for Mobile Robots*. Doctoral Dissertation.

42. Cirillo, Marcello (2010) *Planning in Inhabited Environments: Human-Aware Task Planning and Activity Recognition*. Doctoral Dissertation.

43. Nilsson, Maria (2010) *Capturing Semi-Automated Decision Making: The Methodology of CASADEMA*. Doctoral Dissertation.

44. Dahlbom, Anders (2011) *Petri nets for Situation Recognition*. Doctoral Dissertation.

45. Ahmed, Muhammad Rehan (2011) *Compliance Control of Robot Manipulator for Safe Physical Human Robot Interaction*. Doctoral Dissertation.

46. Riveiro, Maria (2011) *Visual Analytics for Maritime Anomaly Detection*. Doctoral Dissertation.

47. Rashid, Md. Jayedur (2011) *Extending a Networked Robot System to Include Humans, Tiny Devices, and Everyday Objects*. Doctoral Dissertation.

48. Zain-ul-Abdin (2011) *Programming of Coarse-Grained Reconfigurable Architectures*. Doctoral Dissertation.

49. Wang, Yan (2011) *A Domain-Specific Language for Protocol Stack Implementation in Embedded Systems*. Doctoral Dissertation.

50. Brax, Christoffer (2011) *Anomaly Detection in the Surveillance Domain*. Doctoral Dissertation.

51. Larsson, Johan (2011) *Unmanned Operation of Load-Haul-Dump Vehicles in Mining Environments*. Doctoral Dissertation.

52. Lidström, Kristoffer (2012) *Situation-Aware Vehicles: Supporting the Next Generation of Cooperative Traffic Systems*. Doctoral Dissertation.

53. Johansson, Daniel (2012) *Convergence in Mixed Reality-Virtuality Environments. Facilitating Natural User Behavior.* Doctoral Dissertation.

54. Stoyanov, Todor Dimitrov (2012) *Reliable Autonomous Navigation in Semi-Structured Environments using the Three-Dimensional Normal Distributions Transform (3D-NDT).* Doctoral Dissertation.

55. Daoutis, Marios (2013) *Knowledge Based Perceptual Anchoring: Grounding percepts to concepts in cognitive robots*. Doctoral Dissertation.

56. Kristoffersson, Annica (2013) *Measuring the Quality of Interaction in Mobile Robotic Telepresence Systems using Presence, Spatial Formations and Sociometry.* Doctoral Dissertation.

57. Memedi, Mevludin (2014) *Mobile systems for monitoring Parkinson's disease*. Doctoral Dissertation.

58. König, Rikard (2014) *Enhancing Genetic Programming for Predictive Modeling*. Doctoral Dissertation.

59. Erlandsson, Tina (2014) *A Combat Survivability Model for Evaluating Air Mission Routes in Future Decision Support Systems*. Doctoral Dissertation.

60. Helldin, Tove (2014) *Transparency for Future Semi-Automated Systems. Effects of transparency on operator performance, workload and trust.* Doctoral Dissertation.

61. Krug, Robert (2014) *Optimization-based Robot Grasp Synthesis and Motion Control*. Doctoral Dissertation.

62. Reggente, Matteo (2014) *Statistical Gas Distribution Modelling for Mobile Robot Applications*. Doctoral Dissertation.

63. Längkvist, Martin (2014) *Modeling Time-Series with Deep Networks*. Doctoral Dissertation.

64. Hernández Bennetts, Víctor Manuel (2015) *Mobile Robots with In-Situ and Remote Sensors for Real World Gas Distribution Modelling*. Doctoral Dissertation.

65. Alirezaie, Marjan (2015) *Bridging the Semantic Gap between Sensor Data and Ontological Knowledge*. Doctoral Dissertation.

66. Pashami, Sepideh (2015) *Change Detection in Metal Oxide Gas Sensor Signals for Open Sampling Systems*. Doctoral Dissertation.

67. Lagriffoul, Fabien (2016) *Combining Task and Motion Planning*. Doctoral Dissertation.

68. Mosberger, Rafael (2016) *Vision-based Human Detection from Mobile Machinery in Industrial Environments*. Doctoral Dissertation.

69. Mansouri, Masoumeh (2016) *A Constraint-Based Approach for Hybrid Reasoning in Robotics*. Doctoral Dissertation.

70. Albitar, Houssam (2016) *Enabling a Robot for Underwater Surface Cleaning*. Doctoral Dissertation.

71. Mojtahedzadeh, Rasoul (2016) *Safe Robotic Manipulation to Extract Objects from Piles: From 3D Perception to Object Selection*. Doctoral Dissertation.

72. Köckemann, Uwe (2016) *Constraint-based Methods for Human-aware Planning*. Doctoral Dissertation.

73. Jansson, Anton (2016) *Only a Shadow. Industrial Computed Tomography Investigation, and Method Development, Concerning Complex Material Systems*. Licentiate Thesis.

74. Sebastian Hällgren (2017) *Some aspects on designing for metal Powder Bed Fusion*. Licentiate Thesis.

75. Junges, Robert (2017) *A Learning-driven Approach for Behavior Modeling in Agent-based Simulation*. Doctoral Dissertation.

76. Ricão Canelhas, Daniel (2017) *Truncated Signed Distance Fields Applied To Robotics*. Doctoral Dissertation.

77. Asadi, Sahar (2017) *Towards Dense Air Quality Monitoring: Time-Dependent Statistical Gas Distribution Modelling and Sensor Planning*. Doctoral Dissertation.

78. Banaee, Hadi (2018) *From Numerical Sensor Data to Semantic Representations: A Data-driven Approach for Generating Linguistic Descriptions*. Doctoral Dissertation.

79. Khaliq, Ali Abdul (2018) *From Ants to Service Robots: an Exploration in Stigmergy-Based Navigation Algorithms*. Doctoral Dissertation.

80. Kucner, Tomasz Piotr (2018) *Probabilistic Mapping of Spatial Motion Patterns for Mobile Robots*. Doctoral Dissertation.

81. Dandan, Kinan (2019) *Enabling Surface Cleaning Robot for Large Food Silo*. Doctoral Dissertation.

82. El Amine, Karim (2019) *Approaches to increased efficiency in cold drawing of steel wires*. Licentiate Thesis.

83. Persson, Andreas (2019) *Studies in Semantic Modeling of Real-World Objects using Perceptual Anchoring*. Doctoral Dissertation.

84. Jansson, Anton (2019) *More Than a Shadow. Computed Tomography Method Development and Applications Concerning Complex Material Systems*. Doctoral Dissertation.

85. Zekavat, Amir Reza (2019) *Application of X-ray Computed Tomography for Assessment of Additively Manufactured Products*. Doctoral Dissertation.

86. Mielle, Malcolm (2019) *Helping robots help us—Using prior information for localization, navigation, and human-robot interaction*. Doctoral Dissertation.

87. Grosinger, Jasmin (2019) *On Making Robots Proactive*. Doctoral Dissertation.

88. Arain, Muhammad Asif (2020) *Efficient Remote Gas Inspection with an Autonomous Mobile Robot*. Doctoral Dissertation.

89. Wiedemann, Thomas (2020) *Domain Knowledge Assisted Robotic Exploration and Source Localization*. Doctoral Dissertation.

90. Giaretta, Alberto (2021) *Securing the Internet of Things with Security-by-Contract*. Doctoral Dissertation.

91. Rudenko, Andrey (2021) *Context-aware Human Motion Prediction for Robots in Complex Dynamic Environments*. Doctoral Dissertation.

92. Eriksson, Daniel (2021) *Getting to grips with cartons: Interactions of cartonboard packages with an artificial finger.* Doctoral Dissertation.

93. Dinh-Cuong, Hoang (2021) *Vision-based Perception For Autonomous Robotic Manipulation*. Doctoral Dissertation.

94. Akalin, Neziha (2022) *Perceived Safety in Social Human-Robot Interaction*. Doctoral Dissertation.

95. Han Fan (2022) *Robot-aided Gas Sensing for Emergency Responses*. Doctoral Dissertation.

96. Tomic, Stevan (2022) *Human Norms for Robotic Minds*. Doctoral Dissertation.

97. Kondyli, Vasiliki (2023) *Behavioural Principles for the Design of Human-Centered Cognitive Technologies, The Case of Visuo-Locomotive Ewperience*. Doctoral Dissertation.

98. Morillo-Mendez, Lucas (2023) *SOCIAL ROBOTS / SOCIAL COGNITION. Robots' Gaze Effects in Older and Younger Adults.* Doctoral Dissertation.

99. Yang, Yuxuan (2023) *Advancing Modeling and Tracking of Deformable Linear Objects for Real-World Applications.* Doctoral Dissertation.

100. Adolfsson, Daniel (2023) *Robust large-scale mapping and localization*. Doctoral Dissertation.

101. Yang, Quantao (2023) *Robot Skill Acquisition through Prior-Conditioned Reinforcement Learning*. Doctoral Dissertation.

102. Landin, Cristina (2023) *AI-Based Methods For Improved Testing of Radio Base Stations: A Case Study Towards Intelligent Manufacturing*. Licentiate Thesis.

103. Larsson Joakim (*2024) Have you heard about wire?, Monitoring of the wire drawing process*. Doctoral Dissertation.